Pharmacological Research

BCAAs and Di-Alanine supplementation in the prevention of skeletal muscle atrophy: preclinical evaluation in a murine model of hind limb unloading
--Manuscript Draft--

Manuscript Number:	
Article Type:	Research Paper
Keywords:	dietary supplements; branched-chain amino acids; L-Alanine; L-Alanyl-L-Alanine; skeletal muscle atrophy; hind limb unloading
Corresponding Author:	Annamaria De Luca University of Bari Bari, Unspecified ITALY
First Author:	Paola Mantuano
Order of Authors:	Paola Mantuano
	Brigida Boccanegra
	Gianluca Bianchini
	Elena Conte
	Michela De Bellis
	Francesca Sanarica
	Giulia Maria Camerino
	Sabata Pierno
	Ornella Cappellari
	Marcello Allegretti
	Andrea Aramini
	Annamaria De Luca
Abstract:	Skeletal muscle atrophy occurs in response to various pathophysiological stimuli, including disuse, aging, and neuromuscular disorders, mainly due to an imbalance of anabolic/catabolic signaling. Branched Chain Amino Acids (BCAAs: leucine, isoleucine, valine) supplements can be beneficial for counteracting muscle atrophy, in virtue of their reported anabolic properties. Here, we carried out a proof-of-concept study to assess the in vivo/ex vivo effects of a 4-week treatment with BCAAs on disuse-induced atrophy, in a murine model of hind limb unloading (HU). BCAAs were formulated in drinking water, alone, or plus two equivalents of L-Alanine (2ALA) or the dipeptide L-Alanyl-L-Alanine (Di-ALA), to boost BCAAs bioavailability. HU mice were characterized by reduction of body mass, decrease of soleus – SOL – muscle mass and total protein, alteration of postural muscles architecture and fiber size, dysregulation of atrophy-related genes (Atrogin-1, MuRF-1, mTOR, myostatin). In parallel, we provided new robust readouts in the HU murine model, such as impaired in vivo isometric torque and ex vivo SOL muscle contractility and elasticity, as well as altered immune response. An acute pharmacokinetic study confirmed that L-ALA, also as dipeptide, enhanced plasma exposure of BCAAs. Globally, the most sensitive parameters to BCAAs action were muscle atrophy and myofiber cross-sectional area, muscle force and compliance to stress, protein synthesis via mTOR and innate immunity, with the new BCAAs + Di-ALA formulation being the most effective treatment. Our results support the working hypothesis and highlight the importance of developing innovative formulations to optimize BCAAs biodistribution.
Suggested Reviewers:	

Prof. Annamaria De Luca
SEZIONE DI FARMACOLOGIA
DIPARTIMENTO di FARMACIA – SCIENZE del FARMACO
UNIVERSITÀ DEGLI STUDI DI BARI "ALDO MORO"
VIA E. ORABONA, 4
70125 BARI – ITALIA
TEL.: (+39) - 080-544 2245
Email: annamaria.deluca@uniba.it

Bari, June 12th, 2021

To
Prof. Emilio Clementi,
Editor-in-Chief, *Pharmacological Research*

Dear Prof. Clementi,

On behalf of all authors, I shall be obliged if the manuscript entitled "**BCAAs and Di-Alanine supplementation in the prevention of skeletal muscle atrophy: preclinical evaluation in a murine model of hind limb unloading**" would be considered for publication as Original Research Article in *Pharmacological Research*.

The manuscript is not under consideration elsewhere and, if accepted, it will not be published elsewhere in the same form, in English or in any other language, including electronically, without the written consent of the copyright holder. I hereby declare that all contributing authors have seen and approved the submitted version of the manuscript.

We greatly hope that our work would fulfill the requirements to be suitable for publication in *Pharmacological Research*.

Thanking you in advance for kind consideration,
Best regards,

Prof. Annamaria De Luca

Table 1: *Author Checklist for Original Articles to be submitted to Pharmacological Research*

| Questions	reply		
	Yes	*No*	*Not applicable*
Formatting - The submission will automatically be rejected if the first six questions are not marked "yes" (questions 1-6) or "not applicable" (limited to questions 3-6)			
1. Are all tables and figures numbered and appropriately titled with descriptive legends that permit stand-alone interpretation?	✔		
2. Are all data shown on figures and tables mentioned in the text of the Results section?	✔		
3. Are the whole un-cropped images of the original western blots from which figures have been derived shown as supplemental figures?			✔
4. In case of human studies, has specific mention been made of the study compliance with the regulations of the country(ies) in which the study was carried out ?			✔
5. In case of human studies, has the study been registered on an accessible international registry/database of clinical trials (e.g. EudraCT, ClinicalTrials.gov, ChiCTR, ANZCTR, JPRN and the like)			✔
6. In case of studies on animals, is there a statement indicating compliance with regulations on the ethical treatment of animals including identification of the institutional committee that approved the experiments?	✔		
Introduction			
7. Is there a clear statement with background describing the hypothesis being tested by this study?	✔		
8. Are the primary endpoints clearly described?	✔		
Materials and Methods			
9. Are the sources of all materials clearly indicated?	✔		
10. Is(are) the chemical structure(s) of any new compound(s) presented as a figure in the manuscript or referenced in the literature?			✔
11. Are the source(s) and passage number of cell lines indicated?			✔
12. Are the source, catalogue number and lot for commercial antibodies indicated?			✔
13. Are the species, strain, sex, weight and source of the animal subjects provided?	✔		
14. Is the rationale provided for the selection of concentrations, doses, route and frequency of compound administration?	✔		
15. Are quantified results (*e.g.* IC_{50} and/or EC_{50} values) of concentration- and dose-response experiments included in the report?			✔
16. Is the method of anaesthesia described?	✔		
17. Are all group sizes approximately the same?	✔		
18. Were the criteria used for excluding any data from analysis determined prospectively and clearly stated?	✔		
19. Was the investigator responsible for data analysis blinded to which samples/animals represent treatments and controls?	✔		
20. Is the exact sample size (n) for each experimental group/condition clearly indicated in the text and/or on the tables and figures?	✔		

21. Are the reported data displayed as the mean +/- an estimate of variability (SD, SEM) of three or more independent experimental replications?	✔		
22. Is the number of replications used to generate an individual data point in each of the independent experiments clearly indicated?	✔		
23. Were the statistical tests employed to analyse the primary endpoints predetermined as part of the experimental design?	✔		
24. Is the threshold for statistical significance (P value) clearly indicated?	✔		
25. Were the data normalised?	✔		
26. Were post-hoc tests used to assess the statistical significance among means?	✔		
27. Was the study exploratory rather than hypothesis-driven?		✔	
28. Were human tissues or fluids used in this study?		✔	
Results			
29. If western blots are shown, are the following included: i) appropriate loading controls for each western blot, ii) replication data, iii) quantification, and iv) the results of a statistical analysis?			✔
30. Were MIQE guidelines followed in the quantitative analysis and presentation of PCR and RT-PCR findings?	✔		
31. Was a reference standard (positive or negative controls) included in the study to validate the experiment?	✔		
Discussion			
32. Are all the findings considered within the context of the hypothesis presented in the Introduction?	✔		
33. Are the primary conclusions and their implications clearly stated?	✔		
34. Are any secondary endpoints reported and are these sufficiently powered for appropriate statistical analysis?	✔		
35. Are the limitations of the current study or alternative interpretations of the findings clearly stated?	✔		
For Meta-analyses only			
36. Were the PRISMA reporting guidelines and checklist followed in the case of meta-analyses on randomised controlled trials?			✔
37. Were the MOOSE reporting guidelines followed in the case of meta-analyses on observational studies in epidemiology?			✔
38. Was the protocol submitted into the PROSPERO International prospective register of systematic reviews and a registration number obtained?			✔
Conflict of Interest/Financial Support			
39. Is the conflict of interest statement is included in the manuscript?	✔		
40. Are all organisations providing funding for this work listed in the Acknowledgments?	✔		

Feedback/suggestions on the checklist by the author

BCAAs and Di-Alanine supplementation in the prevention of skeletal muscle atrophy

Validation and implementation of the HU mouse model

- Overt atrophy of postural muscles
- Change in gene signature and protein unbalance
- Muscle weakness and stiffness
- Histomorphological alterations
- Defect in innate immune response
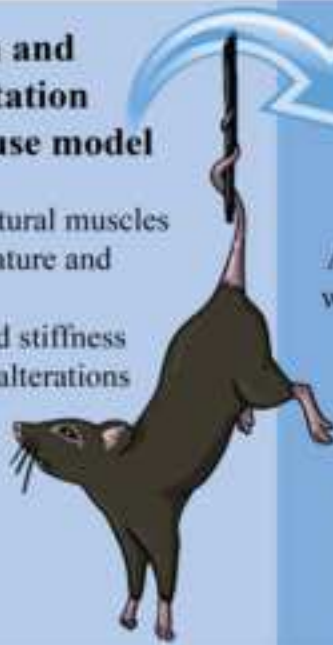
Nutraceutical approach in disuse-related atrophy

BCAAs — Amino acids with anabolic potential

Di-Alanine — Booster of BCAAs bioavailability

4-week treatment:
- Pre-treatment before suspension (2 weeks)
- Administration during suspension (2 weeks)

Results

- Increase of SOL muscle mass, myofibers CSA and total protein content
- Better muscles compliance to stretch
- Reduced expression of atrophy-related genes
- Immuno-protective activity

Original full-length research article

BCAAs and Di-Alanine supplementation in the prevention of skeletal muscle atrophy: preclinical evaluation in a murine model of hind limb unloading

Paola Mantuano[1#] and Brigida Boccanegra[1#], Gianluca Bianchini[2], Elena Conte[1], Michela De Bellis[1], Francesca Sanarica[1], Giulia Maria Camerino[1], Sabata Pierno[1], Ornella Cappellari[1], Marcello Allegretti[2], Andrea Aramini[2]*, Annamaria De Luca[1]*

[1] Section of Pharmacology, Department of Pharmacy-Drug Sciences, University of Bari "Aldo Moro", Orabona 4 - Campus, 70125 Bari, Italy

[2] Research & Early Development, Dompé farmaceutici S.p.A., Via Campo di Pile, s.n.c. 67100 L'Aquila, Italy

[#] These two authors contributed equally to this work

* Corresponding Authors: annamaria.deluca@uniba.it; Tel.: +39 080 5442245; andrea.aramini@dompe.com; tel.: +39 0862 338340.

Abstract

Skeletal muscle atrophy occurs in response to various pathophysiological stimuli, including disuse, aging, and neuromuscular disorders, mainly due to an imbalance of anabolic/catabolic signaling. Branched Chain Amino Acids (BCAAs: leucine, isoleucine, valine) supplements can be beneficial for counteracting muscle atrophy, in virtue of their reported anabolic properties. Here, we carried out a proof-of-concept study to assess the *in vivo/ex vivo* effects of a 4-week treatment with BCAAs on disuse-induced atrophy, in a murine model of hind limb unloading (HU). BCAAs were formulated in drinking water, alone, or plus two equivalents of L-Alanine (2ALA) or the dipeptide L-Alanyl-L-Alanine (Di-ALA), to boost BCAAs bioavailability. HU mice were characterized by reduction of body mass, decrease of soleus – SOL – muscle mass and total protein, alteration of postural muscles architecture and fiber size, dysregulation of atrophy-related genes (*Atrogin-1*, *MuRF-1*, *mTOR*, *myostatin*). In parallel, we provided new robust readouts in the HU murine model, such as impaired *in vivo* isometric torque and *ex vivo* SOL muscle contractility and elasticity, as well as altered immune response. An acute pharmacokinetic study confirmed that L-ALA, also as dipeptide, enhanced plasma exposure of BCAAs. Globally, the most sensitive parameters to BCAAs action were muscle atrophy and myofiber cross-sectional area, muscle force and compliance to stress, protein synthesis via *mTOR* and innate immunity, with the new BCAAs + Di-ALA formulation being the most effective treatment. Our results support the working hypothesis and highlight the importance of developing innovative formulations to optimize BCAAs biodistribution.

Keywords: dietary supplements; branched-chain amino acids; L-Alanine; L-Alanyl-L-Alanine; skeletal muscle atrophy; hind limb unloading.

1

List of Abbreviations

AAs, amino acids; BCAAs, branched-chain amino acids; CK, creatine kinase; CLCN1, chloride voltage-gated channel 1; col1a1, collagen type 1 α 1; col1a3, collagen type 1 α 3; CSA, cross-sectional area; Di-ALA, L-Alanyl-L-Alanine; EAAs; essential amino acids; EDL, extensor digitorum longus; Eln, elastin; GC, gastrocnemius; gCl, chloride ion channel conductance; GO, gene ontology; H&E: hematoxylin & eosin; HPRT1, Hypoxanthine Phosphoribosyl transferase 1; HU, hind limb unloading; IgA, immunoglobulin A; IL-6, interleukin 6; KGF, kilogram/force; L-ALA, L-Alanine; LDH, lactate dehydrogenase; MHC-1/2A/2B, myosin heavy chains 1/2A/2B; MLC-1 and 2, myosin light chains 1 and 2; mTOR, mammalian target of rapamycin; MuRF1, Muscle RING Finger-1; MyoD, myoblast determination protein 1; NMDs, neuromuscular disorders; PEPT1, Peptide transporter 1; PGC-1α - Peroxisome proliferator-activated receptor gamma coactivator 1-α; PK, pharmacokinetics; QUAD, quadriceps; SDH, succinate dehydrogenase; SOL, soleus; SOPs, standard operating procedures; TA, tibialis anterior; TBP, TATA box protein; TGF-β1, Transforming growth factor β 1; TREAT-NMD, Treat NeuroMuscular Disease.

1. Introduction

Skeletal muscle atrophy is defined as a loss of muscle mass leading to a partial or complete decline of muscular function. This clinical condition represents a comorbidity of a large miscellany of diseases and pathophysiological events, including aging (sarcopenia), disuse, cancer (cachexia) and neuromuscular disorders[1]. The severe muscle weakness associated to atrophy, considerably compromises life quality of affected patients, by worsening prognosis and increasing mortality.

Focusing on disuse atrophy, prolonged periods of muscle inactivity (*e.g.* due to bed rest, limb immobilization, mechanical ventilation, coma, etc.), generate a severe reduction of muscle strength and a rapid fatigability[2]. Studies performed on rodent (rats and mice) models of disuse-induced skeletal muscle atrophy via hind limb-unloading (HU)[3,4], evidenced a reduction in skeletal muscle myofibers size and cross-sectional area (CSA), accompanied by an alteration of mitochondrial function, with ROS overproduction and enhancement of oxidative stress[5]. This was accompanied by an increase of chloride ion channel conductance (gCl)[6] and sodium channel expression[7], both hallmark features of fast-glycolytic fibers. Also, in HU rat models, a fiber type switching consisting

2

in a slow-oxidative toward fast-glycolytic transition was recognized, and this was more evident in postural slow-twitch muscle[8,9].

Although the detailed framework of disuse atrophy's etiology is still unclear, the primary reason of muscular tissue depletion is a disequilibrium between anabolic and catabolic events, with the triggering of pathways involved in protein breakdown and a reduction in protein synthesis[3]. Ubiquitin (Ub)-proteasome system, Ca^{2+}-dependent calpains and lysosomal cathepsins are, alone or in synergy, key mediators involved in muscle cells size reduction and impaired capacity of self-renewal, playing a crucial role in primary cellular events like proteolysis and apoptosis[3]. In detail, skeletal muscles cells of HU rodents and immobilized patients, showed an overactivation of Ub-proteasome pathway and the upregulation of Ub-ligases *Atrogin-1* and Muscle RING Finger-1 (*MuRF1*), which are responsible for poly-ubiquitination and subsequent degradation of a plethora of substrates, including myogenic factors (*MyoD*, *myogenin*), structural proteins (*e.g.* myosin heavy chains – *MHC – 1, 2A* and *2B* and myosin light chains – *MLC – 1* and *2*) and proteins involved in glucose metabolism (*e.g.* pyruvate dehydrogenase, glycogenin)[10]. In parallel, it is well-known that the serine/threonine protein kinase mammalian target of rapamycin (*mTOR*) pathway is of utmost importance for regulation of protein synthesis and linked to BCAAs catabolism in health and disease conditions, such as carcinogenesis and cachexia[11,12]. At this regard, it has been established that the mTOR pathway is downregulated during muscle disuse while its upregulation may prevent muscle atrophy *in vivo*[13]. Therefore, targeting one or several of the abovementioned pathways may represent an effective therapeutic strategy to counteract disuse atrophy.

In this frame, nutraceutical compounds and, in particular, amino acids (AAs) with anabolic properties appear as potentially useful adjuvants in the treatment of disuse atrophy. Branched-chain amino acids (BCAAs *i.e.* leucine, isoleucine, and valine) are three essential amino acids (EAAs) commonly recognized as anabolic substances in view of their capacity to stimulate protein

3

synthesis in mammals[14]. In the last decades, BCAAs gained a widespread popularity especially among athletes, both professionals and amateurs, on account of the benefits observed on physical performance after their supplementation. BCAAs mechanism of action is twofold: on one hand, BCAAs (especially leucine) are indeed capable to stimulate protein synthesis activating the *mTOR* signaling pathway; on the other hand, BCAAs also inhibit protein breakdown, by reducing the increase of *Atrogin-1* and *MuRF-1* proteins levels and affecting Ub-proteasome activity[15]. In addition, BCAAs play a role in glucose metabolism, promoting insulin secretion and muscle glucose uptake[16], in order to increase the availability of energetic substrates required for anabolic reactions. Several studies, on both animal models and humans, confirmed the potential of BCAAs in promoting protein synthesis[17,18]. Interestingly, in a very recent work[19], we evaluated the ergogenic effect of BCAAs supplementation in a murine model of physiological exercise and studied the combined effect of increasing doses of L-Alanine (L-ALA). The results showed that BCAAs (in a 2:1:1 ratio), administered for 4 weeks, ameliorated exercise performance, enhanced muscle strength and reduced fatigability with the parallel increase in hind limb muscles' mass. Also, the co-administration of L-ALA, the main amino acid derived from BCAAs catabolism, was confirmed to boost BCAAs bioavailability, with the BCAAs plus ALA in 2:1:1:2 ratio (BCAAs + 2ALA) being the optimal composition, based on pharmacokinetics data and enhancement of BCAAs ergogenic effect. These results, obtained in a physiological condition, suggest that BCAAs supplementation, particularly if combined with L-ALA, could also represent a countermeasure for disuse-induced muscle impairment. However, to date, few preclinical and clinical studies have been conducted to assess the BCAAs effect in relevant animal models or in patients affected by atrophy related conditions[20,21].

With the aim to gain a deeper understanding of the actual effects of BCAAs and L-ALA supplementation in disuse muscle atrophy, we performed a proof-of-concept preclinical study in a

4

murine model of hind limb unloading (HU). HU mice were treated with BCAAs alone, or in combination with the most effective dose of L-ALA. In addition, we wanted to evaluate the efficacy of a new oral mixture based on BCAAs combined with the dipeptide L-Alanyl-L-Alanine (Di-ALA). Di-ALA could, in fact, increase the bioavailability of L-ALA for the fastest rate of intestinal uptake and absorption of dipeptides compared to free amino acids[19,22], in turn potentially enhancing BCAAs bioavailability. Furthermore, Di-ALA is a potent activator of human intestinal oligopeptide transporter (PEPT1) responsible for oligopeptides uptake throughout the brush border membrane of enterocytes[23]. Both potential benefits and safety of BCAAs plus 2ALA or Di-ALA supplementation were evaluated by combining multiple *in vivo* and *ex vivo* endpoints. Thus, our study sought to clarify the real contribution of these amino acid mixtures in muscle atrophy relief, paving the way for the application of recognized nutritional strategies in muscle disorders treatment.

2. Materials and Methods

All the experiments were conducted in conformity with the Italian Guidelines for Care and Use of Laboratory Animals (D.L.116/92) and with the European Directive (2010/63/EU), as well as in compliance with the ARRIVE guidelines. The study was approved by the National Ethics Committee for Research Animal Welfare of the Italian Ministry of Health (authorization no. 271/2019-PR). Being muscle atrophy a condition which is commonly observed in neuromuscular disorders (NMDs), the rigour of the experimental *in vivo* and *ex vivo* procedures was inspired by the international guidelines for preclinical studies in NMDs[24] (http://www.treat-nmd.eu/research/preclinical/dmd-sops/).

2.1 Pharmacokinetic Study

A pharmacokinetic (PK) evaluation of tested amino acids distribution in wild type (WT) mice was conducted in acute conditions[19]. A total of 18 (n = 6 mice *per* group), 10-week-old, male C57BL/6J WT mice (Harlan, Italy) were used. The night before the administration of labelled amino acids, animals were fasted; food was re-inserted in cages 3 hours after amino acid supplementation. For all groups, the administered dose for each of the three BCAAs was as follows: L-Leucine-13C6, 15N: 328 mg/kg; L-Isoleucine-13C6, 15N: 164 mg/kg; L-Valine-13C5, 15N: 164 mg/kg. L-Alanine was added to the BCAAs + 2ALA formulation at the dose of 328 mg/kg; the same dose was used for L-Alanyl-L-Alanine when added to the BCAAs + Di-ALA mixture. For each BCAA, as well as for L-ALA and Di-ALA, the same doses were maintained for the chronic study, obtaining the final dosage (in mg/kg) for each mixture (**Table 1**). Each formulation was prepared dissolving amino acid mixture powder in 1.5 % w/w citric acid aqueous solution. Mice were treated by a single-dose oral gavage (administration volume 15 mL/kg). Plasma was obtained by processing blood samples (50 – 60 μL) collected from the retromandibular vein at increasing time intervals (15 min, 30 min, 1 h, 3 h, 8 h, and 24 h), transferred into labeled tubes and frozen at −80 °C until further PK analysis[19]. Mice were then sacrificed by exsanguination under deep isoflurane anesthesia (EZ-B800 system, WPI, USA). Plasma samples were analyzed by clean-up and derivatization using the EZfaastTM amino acid analysis kit (Phenomenex, Castel Maggiore, BO, Italy) and analyzed by UPLC-MSMS (UPLC Shimadzu model LC-20AD equipped with ABSciex API 4500Q mass spectrometer).

2.2 Animal Groups, Treatments, and Hind Limb Unloading Protocol

A total of 48, 10-week-old, male C57BL/6J WT mice (*Charles River, Calco Italy*) were used to perform the main study. All mice were acclimatized for about 1 week in the animal facility before starting the experimental protocol. Animals were housed in suitable cages (4 mice *per* cage), in a single room where appropriate conditions of temperature (22 – 24 °C), humidity (50 – 60%), and

6

light/dark cycle (12 h/12 h) were constantly maintained for the entire duration of the study. After acclimatization, mice were assigned to each treatment group. Mice cohorts (6 groups, each one composed of n = 8 animals) resulted in being homogeneous for body mass and forelimb grip strength values and were randomly assigned to HU plus each treatment with the BCAAs formulation or with one of the modified formulations (BCAAs + 2ALA, BCAAs + Di-ALA); a group of HU mice was treated with vehicle (filtered tap water), while another cohort of grounded (non-HU) mice was used as control to better evaluate the alteration of specific functional parameters, not yet assessed in the HU mouse model.

Once a week, each formulation was freshly prepared by dissolving the amino acid mixture powder in filtered tap water in order to obtain the desired final dose. The composition (in weight ratio) and the final doses (in mg/kg) are reported in **Table 1**. For BCAAs, a constant ratio of 2:1:1 in L-Leucine, L-Isoleucine, and L-Valine content was maintained.

During the pre-treatment phase (T0 – T2), each amino acid mixture was administered to the animals of respective treatment groups. At T2, the groups of mice treated with mixtures or vehicle underwent a 2-week period of hind limb unloading, in parallel with the treatment protocol. In detail, mice were single housed for 14 days in special cages allowing hind limb suspension with a 30° unloading angle. This is obtained by taping the tail to an adjustable string tied to a hook at the top of the cage. The unloading device movement is on a single axis, which guarantees a free access to food and water, provided *ad libitum*[4].

At the end of suspension, mice were unfastened from the string and sacrificed. The outcome of the 2-week hind limb unloading, and the 4-week treatment protocol was assessed on relevant *in vivo* and *ex vivo* readouts (**Figure 1**). To avoid introducing any bias, all procedures, as well as data collection and analysis, were carried out by blinded experimenters.

Importantly, since a maximum of two mice could be sacrificed *per* day, due the time-consuming *ex vivo* experiments carried out at T4, and with the aim to ensure the same duration of treatment and suspension for all animals, we designed a staggered approach which allowed to introduce two mice *per* day in the experimental protocol since T0.

2.3 *In Vivo* Monitoring and Functional Tests

All mice were longitudinally, non-invasively monitored for health and well-being throughout the entire study period. None of the groups showed signs of pain or distress or macroscopic alterations of vital functions. Body mass variations were regularly assessed at the start of each week during the pre-treatment phase and at the beginning and end of the suspension (**Figure 1**).

2.3.1   Forelimb Grip Strength and Isometric Plantar Flexor Torque

Forelimb grip strength was measured on a weekly basis during the pre-treatment phase, by means of a grip strength meter (Columbus Instruments, USA), according to a validated protocol[25–28]. Maximal force, absolute (expressed in kg force, KGF) and normalized to body mass (in KGF/kg), obtained from five repeated measurements *per* mouse, was used for data analysis[25–28].

At T4, *in vivo* isometric torque produced by hind limb plantar flexor muscles (gastrocnemius – GC, soleus – SOL, plantaris) was assessed using the *1300A 3-in-1 Whole Animal Test System* (Aurora Scientific Inc. – ASI, Aurora, ON, Canada), in mice put under isoflurane inhalation anesthesia, as described in previous work[19,28,29]. Briefly, after prepping the skin of the right hind limb by removing hair and cleaning, the animal was placed supine on a temperature-controlled platform (mod. 809B, ASI) at 36 °C, with the right paw taped to a footplate connected to a dual-mode servomotor (mod. 300C-LR, ASI), forming a 90° angle with the hind limb secured at the knee. Contractions were elicited via percutaneous electrical stimulation of the sciatic nerve, through a pair of needle electrodes (Chalgren Enterprises Inc., CA, USA) connected to a high-power, bi-

phase stimulator (mod. 701C, ASI), in turn controlled by a data acquisition signal interface (mod. 604A, ASI) and by ASI Dynamic Muscle Control software (DMCv5.415). Initial twitches, evoked with 0.2 ms single square wave pulses, were used to adjust the current (from 25 to 40 mA) to maximize torque production. Then, a series of isometric contractions was recorded at increasing frequencies (200 ms pulses at 1, 10, 30, 50, 80, 100, 120, 150, 180, 200 Hz, one every 30 s). Plantar flexor torque obtained at each frequency (N*cm) was calculated via ASI Dynamic Muscle Analysis software (DMAv5.201). Then, torque values were normalized to each mouse body mass (N*mm^3/kg) and used to construct torque – frequency curves[19,28,29].

2.4 *Ex vivo* procedures

2.4.1 Sample Collection, Processing, and Storage

At the end of T4 *in vivo* measurements, two mice *per* day entered the *ex vivo* experimental phase. Body mass and torque final measurements (described in paragraph 2.3.1) were performed on each animal the same day of sacrifice. Mice were anesthetized via intraperitoneal (i.p.) injection with a cocktail of ketamine (100 mg/kg) and xylazine (16 mg/kg). If required, an additional dose of ketamine alone (30 mg/kg) was injected to ensure longer and deeper sedation[25–29]. After the onset of anesthesia (~10 min), pilocarpine hydrochloride (1 mg/kg, Sigma-Aldrich, St. Louis, MO, USA) was injected and after 5 min, and saliva was collected from the oral cavity, transferred in a micro-centrifuge tube containing a protease inhibitor (2% PMSF, Sigma-Aldrich), and kept on ice. Each saliva sample was clarified by centrifugation at 16,000 × g for 10 min at 4 °C. Then, the supernatant was collected and stored at −80 °C until the determination of salivary immunoglobulin A (IgA) levels by enzyme-linked immunosorbent assay (ELISA). Right SOL muscle was carefully removed from the hind limb with tendons intact on both ends and rapidly placed in chambers for isometric and/or eccentric contraction recordings, after which was weighed, snap frozen in N_2, and stored at −80 °C until it was used for mTOR ELISA test. Right GC muscle was weighed, snap frozen in N_2,

and stored at −80 °C until it was used for Real-time PCR (qRT-PCR) experiments. Left GC and SOL muscles were weighed, embedded in a small amount of Tissue-Tek O.C.T. (Bio-Optica, Milan, Italy), immersed in isopentane cooled with liquid nitrogen (N_2) for 60 s, and then stored at −80 °C until further processing for histology and histochemistry. Both right and left hind limb tibialis anterior (TA), extensor digitorum longus (EDL), quadriceps (QUAD), as well as vital organs (liver, heart, kidneys, spleen), were isolated and weighed for a gross examination of toxicity and/or effects. Blood was obtained by cardiac puncture with a heparinized insulin syringe and collected in heparinized tubes (Heparin Vister 5000 U.I./ml). Within 30 min after collection, platelet-poor plasma was obtained after two consequential centrifugation steps (20 min, 2000 × g, 4 °C; 10 min, 10,000 × g, 4 °C), and used fresh to measure creatine kinase (CK) and lactate dehydrogenase (LDH) by spectrophotometry; for each mouse, an aliquot of plasma was stored at −80 °C until further proteomics and gene ontology experiments.

2.4.2 Isometric and eccentric contraction recordings

SOL muscle was securely tied with silk suture 6–0 at proximal and distal tendons during dissection, and then gently removed from the mouse[29]. Two loops were made with each suture to allow placing the muscle into a vertical bath containing 25 ml of isotonic Ringer's solution (in mM): NaCl 148, KCl 4.5, $CaCl_2$ 2.0/2.5, $MgCl_2$ 1.0, NaH_2PO_4 0.44, $NaHCO_3$ 12.0, glucose 5.55, pH 7.2 − 7.4, 27 ± 1 °C) continuously gassed with a mixture of 95% O_2 and 5% CO_2. The distal tendon of the muscle was fixed to a hook at the bottom of the bath, while the proximal tendon was fixed at the top to a force transducer (Dual-Mode Lever System 300C-LR, Aurora Scientific Inc. – ASI, Aurora, ON, Canada). Electrical field stimulation was obtained by two axial platinum electrodes closely flanking the muscle, connected to a high-power bi-phase stimulator (LE 12406, 2Biological Instruments, VA, Italy). The apparatus was equipped with a data acquisition signal interface and software (604A, ASI with Dynamic Muscle Control software DMCv4.1.6, ASI). After equilibration

(~ 30 min), SOL muscle was stretched to its optimal length (L_0, measured with an external caliper), which is the length producing the maximal single contraction (twitch, Ptw) in response to a 0.2 ms square wave 40 – 60 mV pulse. Twitch force and kinetics (Ptw; time to peak, TTP; half relaxation time, HRT) were obtained as mean values from 5 twitches elicited by pulses of 0.2 ms, every 30 s. Tetanic contractions were elicited by applying 1200 ms trains of 2.0 ms pulses at increasing frequencies (10, 20, 40, 60, 80, 100, 120, 140, 180, 200 Hz), every 2 min. Maximal tetanic force (P0) was usually recorded at 140 – 180 Hz. Then, the muscle was subjected to a series of 10 eccentric contractions, every 30 s. Briefly, an initial 300 ms isometric contraction was elicited, followed by a stretch of 10% L_0 at a speed of $1L_0$ s^{-1} imposed for the last 200 ms. The progressive decay in isometric force at 5th and 10th pulse was calculated as the percentage of reduction in force vs. the 1st pulse. Two tetanic stimuli (120 Hz, 500 ms) were elicited 4 and 30 min after the eccentric contraction protocol, to calculate the recovery from the stretch-induced force drop vs. the tetanic force registered before the protocol started, as well as muscle compliance to stretch. Data were analyzed by Dynamic Muscle Analysis software v3.2 (ASI); specific Ptw and P0 were obtained by normalizing absolute values to muscle cross sectional area according to the equation: $sP = P/(Mass/L_f*D)$, where P is absolute tension, Mass is muscle mass, D is density of skeletal muscle (1.06 g/cm^3), and L_f is obtained multiplying L_0 by previously determined muscle length to fiber length ratios (0.71 for SOL)[25–27,29].

2.4.3 Muscle Histology and Histochemistry

Serial cross-sections (8 μm thick) from each frozen right GC and SOL muscles were transversally cut into a cryostat microtome set at −20 °C (HM 525 NX, Thermo Fisher Scientific, Waltham, MA, USA). Slides (Superfrost Plus, Thermo Fisher Scientific) were stained with different methods. Classical histological hematoxylin and eosin staining (H&E; Bio-Optica) was used to estimate GC and SOL muscles architecture and to calculate the area of damage and regeneration (including

11

necrosis, inflammation, non-muscle areas, centronucleation) on the total area of muscle cross-section[19,26–28]. Histochemistry for the mitochondrial marker succinate dehydrogenase (SDH; Bio-Optica), was used to evaluate the percentage (%) of each fiber phenotype (slow oxidative, intermediate, fast non-oxidative), as well as the mean cross-sectional area (CSA, in μm^2) for each fiber subtype. Muscles morphological features were identified using digital images, acquired with a bright-field microscope (CX41, Olympus, Rozzano, Italy) and an image capture software (ImageJ, Olympus). Morphometric analysis was performed on at least five non-overlapping fields (10× magnification for GC, 20× for SOL) of total and constant transverse muscle section[19,26–28].

2.4.4 Isolation of Total RNA, Reverse Transcription, and qRT-PCR

For each mouse, total RNA was isolated from frozen left GC muscle with Trizol (10296028, Life Technologies, CA, USA) and quantified by spectrophotometry (ND-1000 NanoDrop, Thermo Fisher Scientific). Reverse transcription was performed as described elsewhere[19,26,27]. qRT-PCR was performed using the Applied Biosystems Real-Time PCR 7500 Fast system (Thermo Fisher Scientific). Each reaction, carried out in duplicate, consisted in 8 ng of cDNA; 0.5 μL of TaqMan Gene Expression Assays; 5 μL of TaqMan Universal PCR master mix No AmpErase UNG (2x) (C.N. 4324018); and nuclease-free water, not DEPC220 treated (C.N. AM9930; all from Thermo Fisher Scientific), for a final volume of 10 μL. RT-TaqMan-PCR conditions were as follows: step 1: 95 °C for 20 s; step 2: 95 °C for 3 s; step 3: 60 °C for 30 s; steps 2 and 3 were repeated 40 times. Average mRNA expression of target genes was normalized to the mean of three housekeeping genes: *β-actin*, Hypoxanthine Phosphoribosyl Transferase 1 (*HPRT1*), and TATAbox Binding Protein (*TBP*) and quantified by the $2^{\Delta\Delta ct}$ method[30]. TaqMan Hydrolysis primer and probe gene expression assays were ordered with the following assay IDs: *β-actin*: Mm00607939_s1; *HPRT1*: Mm00446968_m1; *TBP*: Mm01277042_m1; *Atrogin-1*: Mm00499523_m1; Muscle RING-finger protein-1 (*MuRF-1*): Mm01185221_m1; Mammalian Target Of Rapamycin (*mTOR*):

12

Mm00444968_m1; *Cathepsin-L*: Mm00515507_m1; *Myostatin*: Mm01254559_m1; *Follistatin*:

Mm00514982_m1; *Elastin*: Mm0054670_m1; Collagen type I α1 (*col1a1*): Mm00801666_g1; Collagen

type I α3 (*col1a3*): Mm01254476_m1; Myosin Heavy Chain (*MHC1*): Mm00600555_m1; Myosin

Heavy Chain 2A (*MHC 2A*): Mm00454982_m1; Myosin Heavy Chain 2B (*MHC 2B*); interleukin 6

(*IL-6*): Mm00446190_m1; Transforming Growth Factor β1 (*TGF-β1*): Mm01178820_m1; *PGC-1α*:

Mm01208835_m1; *CLCN1*: Mm00658624_m1; *β-Dystroglycan*: Mm00802400_m1.

2.4.5 Determination of CK and LDH Plasma Levels

The enzymatic activity of CK and LDH in plasma samples (in U/L) was determined using specific

commercially available diagnostic kits (CK NAC LR and LDH LR, SGM, Rome, Italy). Both the

assays required the use of a spectrophotometer (Ultrospec 2100 Pro UV/Visible, Amersham

Biosciences, Little Chalfont, United Kingdom) set to a wavelength of 340 nm at 37 °C, and were

performed according to the manufacturer's instructions[19,25–29].

2.4.6 Determination of Salivary IgA Levels

Salivary IgA levels were determined using a commercial ELISA kit (Mouse IgA Ready-SET-Go!

ELISA kit, eBioscience, Vienna, Austria), according to the manufacturer's protocol[19,31]. Both

absolute values (ng/ml) and those normalized to total protein content (ng/µg) were measured via a

microplate reader (Victor 3V, Perkin Elmer, Waltham, MA, USA), set to 450 nm, RT.

2.4.7 Determination of mTOR protein levels

Total mTOR protein levels were measured in frozen SOL muscle tissue via ELISA (Mouse mTOR

SimpleStep ELISA® Kit ab206311, Abcam, UK), according to the manufacturer's instructions and

by using provided reagents for both preparation of tissue homogenates and assay. The optical

density of each well was determined, using a Victor 3V microplate reader set to 450 nm, RT. A

323 standard curve was generated for relative quantification. mTOR levels were expressed as pg on μg

324 total protein.

2.4.8 Proteomics and Gene Ontology analysis

326 Plasma proteome analysis was conducted to detect differentially expressed proteins in non-HU

327 animals and in HU mice treated with vehicle, BCAAs and BCAAs + Di-ALA (n = 3 samples *per*

328 group). Proteins were identified and characterized by bottom-ups techniques, that consisted in

329 digestion by proteolytic enzymes. The resulting peptides were separated by reverse-phase

330 chromatography by using a HPLC Ultimate 3000 (Thermo Fisher Scientific) coupled to a SANIST-

331 electrospray ionization (ESI) mass spectrometer and analyzed according to the protocol described

332 in previous study[32]. Raw files were analyzed by database search and *de novo* sequence approaches,

333 and the final protein identification was carried out by SwissProt database by using the murine

334 taxonomy. A focused Gene Ontology analysis was performed towards human homology using

335 SANIST-GO algorithm, and the obtained data were visualized with the NaviGO software

336 (https://kiharalab.org/web/navigo/views/goset.php).

2.4.9 Statistics

338 All data were expressed as mean ± standard error of the mean (SEM). Multiple statistical

339 comparisons between HU groups (vehicle, BCAAs, BCAAs + 2ALA, BCAAs + Di-ALA) were

340 performed by one-way analysis of variance (ANOVA), with Dunnett's test post hoc correction, and

341 Bonferroni post hoc test for PK data, when the null hypothesis was rejected ($p < 0.05$). This allowed

342 the evaluation of intra- and inter-group variability, as well as inter-group statistical comparison,

343 while controlling the experiment-wise error rate for false positive (type I error). Unpaired

344 Student's t-test was used for single comparisons between two individual means, uniquely to

345 address differences between untreated HU vs. non-HU control mice. All data followed with good

14

approximation a normal distribution, being included in the 95% confidence interval of the mean; this generally allows for the clear identification of outliers, if any, and for the application of statistical analyses described above. No outliers were found during the present study and missing data in the results were related only to overt technical issues during the experiments, which led to the exclusion of those specific samples from the analysis[19]. The researchers were blinded to experiments, data collection, and analysis.

Whenever possible, the recovery score, an objective index that directly indicates how much of the deficit is recovered (%) by a treatment [26,33], was calculated for quantitatively measurable outcomes according to TREAT-NMD SOPs, as follows:

$$\text{Recovery score} = \frac{(\text{treated HU mice} - \text{untreated HU mice})}{(\text{control mice} - \text{untreated mice})} \times 100$$

357 ## 3. Results

3.1 Pharmacokinetic data

359 All main pharmacokinetic parameters, BCAAs plasma areas under the curves for the time interval

360 $0 - 24h$ (AUC_{0-24h}, µg/ml*min), maximal concentration (C_{max}, µg/ml), time for maximal

361 concentration (T_{max}, min), and mean residence time (MRT, min), were evaluated after mixtures'

362 administration. Particularly, for AUCs (**Table 2**), the BCAAs + 2ALA group showed a trend

363 toward increase in the exposure of all BCAA, that was statistically significant for L-Valine, whilst

364 comparable values were observed in the BCAAs + Di-ALA group.

365 In parallel, a significant increase of MRT for all the three branched amino acids was observed in

366 the BCAAs + Di-ALA group compared both to BCAAs and BCAAs + 2ALA group (**Table 3**).

3.2 *In vivo* data

368 Values for mice body mass (BM; g), longitudinally monitored from T0 to T4, are shown **Figure 2A**.

369 Prior to hind limb unloading (T0 – T2), BM resulted homogeneous among all mice groups. At T4,

370 final time point after the suspension protocol, a significant difference in BM values was observed

371 between non-HU and HU animals, with no variations induced by the formulations.

372 Forelimb grip strength was assessed weekly, prior to hind limb unloading (at T0, T1, and T2). All

373 mice groups exhibited comparable values for maximal forelimb force, either absolute or

374 normalized to BM (**Suppl. Figure 1A and B**, respectively) from T0 to T2.

375 Isometric plantar flexor torque (N*mm/kg) was measured at T4. As shown in **Figure 2B**, non-HU

376 mice produced the highest torque–frequency curve, with untreated HU mice showing significantly

377 lower values from the stimulation frequency of 80 Hz onwards. A slight improvement in plantar

378 flexor torque was observed in all three treated HU mice groups.

16

3.3 *Ex vivo* data

3.3.1 Mass of Hind Limb Muscles and Vital Organs

As shown in **Figure 3**, BM-normalized SOL muscle mass was significantly reduced in untreated HU mice vs. the non-HU condition. A remarkable protective effect on HU-induced SOL muscle atrophy was exerted either by BCAAs + 2ALA or BCAAs + Di-ALA, with a recovery score of + 65% and + 52% respectively, whilst no amelioration was induced by BCAAs alone. The mass of other major hind limb muscles (GC, TA, EDL, QUAD), as well as of vital organs (liver, heart, kidneys, spleen), normalized to each mouse BM (mg/g) are shown in **Table 4**. No significant differences in muscles and organs mass values were found between non-HU and untreated HU animals, except for an increase observed for kidneys ($p > 0.004$); no modifications were induced by any mixture.

3.3.2 SOL muscle isometric and eccentric contraction parameters

Data from isometric and eccentric contraction recordings performed *ex vivo* in isolated SOL muscles from all mice cohorts are shown in **Figure 4**. About single twitch contraction kinetics (**Figure 4A**), a significant reduction in TTP (ms) was observed in vehicle-treated HU mice compared to non-HU animals suggesting a modulation of calcium homeostasis and, possibly, a slow-to-fast transition in SOL fibers. The TTP shortening decrease was remarkably counteracted in HU mice treated with each formulation, which exhibited recovery scores ranging from + 51% to + 65% toward non-HU TTP value. The differences in contraction kinetics were, however, less appreciable in terms of twitch half relaxation time (HRT; ms) (**Figure 4A**).

Focusing on SOL muscle isometric force measurements, vehicle-treated HU mice exhibited a drastic, statistically significant, reduction in maximal specific twitch (**Figure 4B**; sPtw, in kN/m^2) and tetanic force (**Figure 4C**; sP0, in kN/m^2) compared to non-HU, while no modifications were found in two indices related to calcium homeostasis, sPtw/sP0 ratio and Hz50 (*i.e.* frequency at

17

which 50% of maximal specific tetanic force is produced) (data not shown). Both force indices were

remarkably improved by ALA-containing formulations, and particularly by BCAAs + Di-ALA

(with a recovery score of + 67% for sPtw and + 42% for sP0), while no benefit was exerted by

BCAAs alone. SOL muscle compliance to stretch in response to a series of 10 eccentric contractions

was measured as muscle stiffness (mN/mm^3). As shown in **Figure 4D**, muscles from untreated HU

animals were significantly less compliant to stretch compared to non-HU ones. Also in this case,

the BCAAs + Di-ALA combination was the most effective in ameliorating SOL muscle response to

eccentric contractions, with recovery scores $\leq$ + 71%, followed, to a lesser extent, by BCAAs +

2ALA; mice treated with BCAAs showed stiffness values almost comparable to vehicle-treated

ones. In parallel, no significant variations among groups were observed in terms of force drop or

recovery after the eccentric contraction protocol (data not shown).

3.3.3 Muscle Histology Characterization and Myofiber Type Classification

Results from the histological evaluation of SOL muscle architecture by means of hematoxylin and

eosin (H&E) staining are reported in **Figure 5A** and **Table 5**. Qualitative analysis revealed a

considerable alteration in muscle architecture in untreated HU mice, corroborating the evidence

that SOL muscle was markedly affected by the unloading protocol. These observations were

confirmed by quantitative morphometric analysis (**Table 5**), with vehicle-treated HU mice

showing a significant increase in the percentage of total area of damage with respect to non-HU

animals and a substantial increment in non-muscle areas (*i.e.*, percentage of fibrotic and/or adipose

tissue). SOL muscles from treated HU animals exhibited a qualitative amelioration of muscle

architecture (**Fig. 5A**), paralleled by a trend toward reduction in percentage of total damage and

non-muscle tissue (**Table 5**).

The analysis of SOL muscle fiber phenotype, assessed by histochemistry for succinate dehydrogenase (SDH), are shown in **Figure 5B – D**. The number of slow and intermediate fibers, expressed as percentage of total fiber number, did not display any significant variation between mice cohorts, showing a similar fiber type distribution (**Figure 5C**). A significant decrease in both slow and intermediate myofibers' cross-sectional area (CSA, μm^2) was observed in the HU + vehicle group compared to the non-HU counterpart (**Figure 5D**), with only BCAAs + Di-ALA partially protecting from this decline.

Representative GC sample images stained with H&E from all experimental groups are shown in **Figure 6A**. A significant increase in the percentage of non-muscle area was found in vehicle-treated HU vs. non-HU mice (**Table 5**), showing that GC was also affected by the hind limb unloading protocol. Interestingly, the BCAAs + Di-ALA combination was able to reduce the percentage of non-muscle area more effectively than the other mixtures (**Table 5**).

The histochemistry for SDH (**Figure 6B**) evidenced a homogeneous distribution of slow, intermediate, and fast myofibers in GC muscles from all mice cohorts. As for SOL muscle, the mean CSA for all fiber types (**Figure 6C**) was significantly reduced in HU + vehicle compared to non-HU mice. All mixture-treated groups showed a trend toward increase in GC muscle mean myofiber CSA, with recovery scores ranging from + 35% to + 45%.

3.3.4 Gene Expression Analyses

The results of gene expression experiments performed by qRT-PCR in GC muscles from all mice cohorts are shown in **Figure 7**. The expression profile of *Atrogin-1* and *MuRF-1*, two genes that are pivotal in controlling muscle atrophy progression, was remarkably increased in vehicle-treated HU mice muscles compared to non-HU ones. A trend to mitigate *MuRF-1* upregulation was observed in all formulation-treated groups. Similarly, BCAAs and BCAAs + Di-ALA partially

counteracted *Atrogin-1* gene induction (**Figure 7, upper panel**). Gene expression analysis of *mTOR*,

the master regulator of protein synthesis, revealed a significant decrease of its levels in vehicle-

treated HU vs. non-HU animals, in accordance with the severe impairment of *mTOR* signaling

pathway in atrophic muscles described in literature[13]. Notably, all amino acid mixtures were able

to revert this outcome, by inducing a significant enhancement of *mTOR* expression (**Figure 7,**

upper panel). A trend toward an increased expression of *myostatin*, a negative modulator of

muscle mass growth, was observed in HU vs. non-HU mice. BCAAs + Di-ALA, as well as BCAAs

alone, significantly reduced *myostatin* expression in treated mice muscles compared to vehicle,

whereas BCAAs + 2ALA treatment had no relevant effect. *Follistatin* expression, a powerful

antagonist of *myostatin*, reflected the trend observed in *myostatin* expression pattern in a mirrored

form. Consequently, a decrease in *follistatin* gene levels was found in untreated HU vs. non-HU

ones, whilst a marked increase, although not significant, was observed in treated HU mice; this

was more evident in BCAAs + Di-ALA and BCAAs group (**Figure 7, lower panel**).

To better evaluate the static and elastic features of myofibers, the expression ratio of *Eln / (col1a1 +*

col1a3) was calculated. The ratio was significantly decreased in untreated HU vs. non-HU mice,

suggesting a reduced elastic capacity of myofibers due to disuse. Mixtures' administration in HU

mice inverted this result, with an increased ratio due to a greater contribution of elastic and/or to a

reduction of static components (**Figure 7, lower panel**).

Hind limb unloading did not affect the expression of myokine *IL-6* gene. By contrary, mixtures'

administration significantly reduced *IL-6* expression with respect to the HU + vehicle group

(**Figure 7, lower panel**). Finally, and in line with the results obtained by histochemistry for SDH,

no significant change was observed in the *MHC 1 / (MHC 2A + 2B)* ratio among mice cohorts,

reinforcing the lack of disuse-related myofiber type switch. Accordingly, no change was observed

in *CLCN1* channel expression and in the metabolic master regulator *PGC-1α*; in parallel, no

remarkable changes were found in the expression of *cathepsin L*, a gene encoding for the lysosomal

endopeptidase, as well as of pro-fibrotic *TGF-β1* and integrity sarcolemmal biomarker *β-dystroglycan* (**Suppl. Figure 2**).

3.3.5 Biomarkers Related to Protein Synthesis, Immune Response and Muscle Damage

To assess the impact of hind limb unloading and amino acid formulations on protein synthesis, the

expression of mTOR protein, absolute (ng/ml) and normalized to total protein content (pg/µg), was

measured by ELISA in SOL muscles of HU mice, either treated or not, compared to non-HU ones

(**Figure 8A – C**). As expected, total protein content (mg/ml) (**Figure 8A**) was significantly reduced

in SOL muscles from vehicle-treated HU mice with respect to non-HU mice. Interestingly, mice

groups treated with the formulations were markedly protected from SOL muscle protein decline,

with recovery scores ranging from + 77% to + 50%. As shown in **Figure 8B**, this trend was partially

confirmed by the analysis of mTOR absolute protein levels in SOL muscle, which showed a

significant reduction in untreated HU mice vs. non-HU ones; however, despite the positive effect

observed on mTOR gene expression levels, none of the formulations was able to protect from

mTOR protein decrease on either absolute or mostly on normalized mTOR values (**Figure 8B, C**).

Salivary IgA levels, absolute (ng/ml) and normalized to total protein content (ng/µg) are shown in

Figure 8D and **E**, respectively. Untreated HU mice showed a severe decrease in concentration of

salivary IgA, either absolute or normalized, in line with previous observations concerning the

impairment of immune response in other murine models of hind limb unloading[34]. HU mice

treated with each formulation displayed variable results. Nonetheless, BCAAs + Di-ALA

supplementation was highly effective in preserving both absolute and normalized salivary IgA

levels, which almost overlapped those found in non-HU mice samples (recovery score + 97% and +

94%, respectively).

Finally, plasma levels (U/L) of CK and LDH enzymes, biochemical markers of muscle damage and metabolic sufferance, respectively, did not show any significant modification among mice cohorts (**Suppl. Table 1**).

3.3.6 Plasma proteomics and Gene Ontology Analysis

With the aim to find potential biomarkers, and after evaluating gene expression in GC muscle, we decided to perform a whole plasma proteome analysis in non-HU animals, and HU mice treated with vehicle, BCAAs and BCAAs + Di-ALA, as well as the relationship between genes and GO terms (Gene Ontology). A blinded large-scale data analysis of plasma samples allowed to identify 23 proteins, of which three resulted to be more abundant and treatment-sensitive (filamin-B, midasin and myoferlin), as shown by an increased detection intensity measured as spectral counts (**Figure 9**). Of particular interest, was the change observed in myoferlin, a multifunctional protein involved in membrane-fusion events in response to muscle injury in both myoblasts and mature myofibers [35], and found to be increased in damaged muscles, *e.g.* in animal models of muscular dystrophy [36,37]. Myoferlin resulted to be significantly increased in vehicle-treated HU mice compared to non-HU. Both BCAAs and BCAAs + Di-ALA induced a significant reduction in myoferlin amount in HU mice with respect to untreated counterparts.

Less evident was the effect of HU on plasma levels of filamin B, a cytoplasmic signaling protein, and midasin, a less characterized protein, while both proteins were modified by BCAAs and BCAAs + Di-ALA, suggesting a direct yet complex relationship with BCAAs supplementation.

In the light of these results, a Gene Ontology (GO) profiling was performed for human homologous of these three proteins, in order to establish a relationship between their encoding genes, as well as their association with a specific GO term (class). The results evidenced a strong correlation between genes O75369 (filamin-B), Q9NU22 (midasin) and Q9NZM1 (myoferlin), and

22

517 that such correlation was associated with the GO term GO:0016020, identifying the structural

518 biological domain Cellular Component - Cell membrane.

4. Discussion

520 In the last decades, the search for increasingly reliable animal models and rigorous experimental

521 protocols as a platform for preclinical research in the field of neuromuscular degenerative

522 disorders, is assuming ever greater importance. Robust and accurate preclinical data indeed allow

523 to improve translatability to clinics, strongly reducing costs and avoiding the involvement of

524 patients in inconsistent trials[24].

525 The present work supports the validity of the hind limb unloaded (HU) mouse, a murine model of

526 disuse atrophy, for translational research on this common muscle-wasting condition. Furthermore,

527 we provided new robust readouts on this animal model of interest for translational research.

528 In the first place, we confirmed that the 2-week protocol of hind limb suspension induced a

529 significant reduction of body mass in mice, hallmark of atrophic conditions that is also typical in

530 humans[1]. Moreover, the decrease in SOL muscle mass we found in HU animals is in line with the

531 primary involvement of this postural muscle in unloading-induced atrophy in mice[3,4]. At the

532 morphological level, this was paralleled by a severe impairment of myofibers architecture in SOL

533 muscle, and, to a lesser extent, in GC muscle of unloaded mice, with substantial evidence of

534 muscle tissue damage and loss, both consistent with the atrophic process. No evident signs of

535 increased inflammatory cells infiltrates were observed, according to the finding that inflammation

536 is not the leading mechanism underlying disuse atrophy[38]. Accordingly, the GC muscle expression

537 of *IL-6* gene, encoding for a pro-inflammatory cytokine that acts as anti-inflammatory myokine

538 when synthetized by muscle cells, was not affected by the suspension protocol.

Also, SDH immunostaining for fiber typing highlighted a significant reduction in mean CSA of all myofiber types either in SOL or GC muscle from HU animals, as described elsewhere[3,4]. Importantly, this staining did not reveal any overt slow-to-fast myofiber shift in these two muscles. This was supported by the lack of modifications in the expression of myosin heavy chain isoform genes and other phenotype marker genes shown by qRT-PCR experiments in GC muscle. This results is in agreement with previous data obtained from mice subjected to a 2-week suspension, in which disuse-related slow-to-fast transition is less evident with respect to HU rats[3,4,8,9]. In this regard, it is important to underline that the shift is mainly an adaptive mechanism to the change of activity, rather independent from the atrophy-related damage[39]. This may be influenced either by the duration of the suspension protocol or by the specific mouse strain selected for this study. In fact, previous findings demonstrated that expression of MHC isoforms could be determined by genetic background[40].

We also confirmed a dysregulation of most pivotal signals involved in muscle atrophy progression, and particularly *Atrogin-1* and *MuRF-1* genes, which were highly expressed in GC muscles from HU mice[3]. In addition, the expression of *mTOR* gene and protein was severely downregulated in GC and SOL muscles, respectively, accompanied by a significant drop of SOL total protein content. These data support the impaired balance between protein synthesis and protein breakdown extensively described in atrophic muscles. In parallel, *myostatin*, a negative modulator of muscle mass, tended to be overexpressed at the transcript level in unloaded mice, suggesting the setting up of the early stage of the atrophic process. Thus, the 2-week suspension protocol triggered a range of genomic signals remodeling, giving rise to the typical functional and macroscopic pattern of the atrophic condition.

Importantly, our first-time assessment of *in vivo* torque in hind limb unloaded mice, provided direct evidence of a severe muscle force loss of plantar flexor muscles, increasing our knowledge about the neuromuscular impairment of this animal model.

The HU-induced, muscle-specific alteration was also evident on SOL muscle function. In fact, unloaded mice displayed a faster kinetics *ex vivo*, as evidenced by the decrease in single twitch TTP, likely in relation to the early increase of gCl, described in previous work[6]. This latter is a process that may anticipate phenotype transition and is associated to both change in calcium homeostasis and mechanical trigger. The parallel absence of modifications observed in HRT, may imply a lack of change or a compensatory mechanism of Sarco-Endoplasmic Reticulum Calcium ATPase (SERCA)[25–29,33]. In agreement with the working hypothesis, SOL muscle was also less compliant to stretch in response to eccentric stimulation. This latter observation was supported by qRT-PCR results, showing a significant reduction of *Eln / (col1a1 + col1a3)* ratio in GC of HU mice.

Interestingly, we disclosed that the levels of salivary IgA, the most prevalent immunoglobulin isotype in the oral cavity, were decreased in HU mice, revealing a severe impairment of the innate immune response, according to a published study describing an increased susceptibility to infections in other HU rodent models[41].

Finally, our plasma proteome analysis revealed a significant increase of myoferlin levels in unloaded mice, according to previous observations in other experimental models of muscle-wasting conditions[37,42]. This result confirmed the role of this protein as a sensitive index of muscle damage, corroborating its potential as new, disease-relevant preclinical biomarker.

A nutraceutical approach in disuse-related atrophy may represent an innovative strategy to counteract muscle wasting in affected patients. BCAAs, due to their claimed anabolic potential, provide a suitable choice in the multifaceted field of nutritional supplements. On the other hand,

the lack of robust evidence on safety and efficacy of BCAAs in muscle-wasting conditions represents, undoubtedly, a remarkable hindrance in the usage of these AAs in patients. Therefore, the goal of our study was to contribute filling this gap, by evaluating in the HU mouse the effects of BCAAs alone or combined with two equivalents of L-Alanine (2ALA), an amino acid already proven to boost BCAAs bioavailability in physiological conditions[19], and a novel mixture in which the same theoretical amount of dipeptide Di-ALA was added, in the view of a possible faster intestinal dipeptide absorption[23].

Our PK analysis confirmed that L-ALA, also as dipeptide, enhanced plasma exposure of BCAAs, and their consequent bioavailability. Both L-ALA enriched formulations protected SOL muscle from disuse-induced atrophy, more than BCAAs alone. This finding ties well with our recently published study, in which the BCAAs + 2ALA mixture was highly capable to increase SOL muscle mass in a murine model of physiological exercise[19], supporting the working hypothesis that the combination of L-ALA with BCAAs boosts these amino acids exposure and anabolic properties.

In line with this, we found that the BCAAs + Di-ALA formulation induced a partial recovery of myofiber CSA in SOL muscle of unloaded mice. Notably, GC muscle appeared more sensitive to the three mixtures action, with a greater preservation of mean fiber CSA.

The protection observed at the morphological level, was mildly detectable on *in vivo* plantar flexor torque, whilst a remarkable muscle-specific effect was observed on contractile indices of isolated SOL muscle *ex vivo*. All mixtures were able to preserve the slow kinetics of SOL myofibers, with a TTP value similar to that of grounded mice. Interestingly, also in this case, only the L-ALA-enriched mixtures demonstrated a beneficial effect in terms of twitch and tetanic force, with the following order of potency: BCAAs + Di-ALA > BCAAs + 2ALA > BCAAs. Furthermore, the same trend was observed in the amelioration of muscle stiffness in response to stretch. Accordingly, GC

26

muscle gene expression analysis showed an increase in *Eln / (col1a1 + col1a3)* ratio in treated mice, supporting the recovery of myofibers elastic components.

Overall, gene expression profile of HU treated mice revealed a complex framework, with mixed results between groups. Some mixtures had indeed the ability, more than others, in reducing the expression of atrophy-related genes (*Atrogin-1*, *MuRF-1*), as well as *myostatin* involved in regulation of muscle mass growth. In the latter case, it should be noted that the mix with BCAA + dipeptide Di-ALA appeared to be more effective among the mixtures. However, the effect on *mTOR* expression was clearly defined, with an upregulation of this gene which was remarkable and homogeneous among all mixtures. This evidence was corroborated by the raise of total protein content in SOL of all treated mice, although the mTOR protein levels in the same muscle was not markedly increased. Moreover, all mixtures, in particular BCAAs + Di-ALA remarkably diminished basal *IL-6* gene expression, confirming our previous results[19]. However, the possible role of the myokine in treated HU mice remains to be understood.

In parallel, despite the high variability among HU treated groups, the BCAAs + Di-ALA formulation was the most effective in restoring IgA salivary levels up to control ones, confirming the immuno-protective activity of these amino acids[19].

Also, the significant reduction of myoferlin levels found in treated mice plasma samples by proteomic analysis, further supported the protective effect exerted by these formulations, and particularly by BCAAs combined with Di-ALA, on damage-related markers in atrophic muscles and corroborate the previously underlined interest of myoferlin as novel and treatment sensitive biomarker.

Globally, the results from proteomics and Gene Ontology profiling in plasma samples, provided interesting hints on potentially relevant biomarkers associated with the effect of BCAAs treatment

on muscular tropism. The observed effect on the expression of filamin-B, midasin, and especially of myoferlin, set the basis for further investigations about their involvement in preserving sarcolemmal integrity, and their role as mediators in chronic muscular pathologies and skeletal malformations.

5. Conclusions

Our results corroborate the hypothesis that BCAAs-based supplements may be useful to protect skeletal muscles in a condition of disuse atrophy, also highlighting the importance of developing innovative formulations able to increase BCAAs bioavailability and to prolong BCAAs residence time. Encouraging results emerged on relevant markers and readouts of disease progression on both SOL and GC muscles, particularly regarding the new formulation based on the combination of BCAAs with the dipeptide Di-ALA.

Our findings pave the way to the appropriate use of nutritional supplements in muscle-wasting conditions, and particularly in disuse-atrophy, for which currently a few and controversial therapies are available, *i.e.* physical, ultrasound, or electrical stimulation, and pharmacological interventions require the use of unwieldy drugs with relevant side effects (*i.e.* β2-agonists, growth hormone, selective androgen receptor modulators, SARMs). This explorative research may represent a solid starting point for clinical investigations aimed to support the use of these specific amino acids as adjuvants in the treatment of disuse atrophy and other muscle-wasting conditions, such as cachexia or age-related sarcopenia.

Additional Information

Patents

The compounds used for this study were provided by Dompé farmaceutici S.p.A. with patent application no. 102019000010401.

Funding

Acknowledgments

Conflicts of Interest

The funders conducted the acute pharmacokinetic study (paragraphs 2.1 and 3.1), as well as the plasma proteome and gene ontology study (paragraphs 2.4.8 and 3.3.6), and they had a supporting role in study design, as well as in manuscript revision. All other authors declare no conflict of interest.

REFERENCES

1. Evans WJ. Skeletal muscle loss: cachexia, sarcopenia, and inactivity. *Am J Clin Nutr*. 2010;91(4):1123S-1127S. doi:10.3945/ajcn.2010.28608A

2. Dirks ML, Wall BT, van Loon LJC. Interventional strategies to combat muscle disuse atrophy in humans: focus on neuromuscular electrical stimulation and dietary protein. *J Appl Physiol*. 2017;125(3):850-861. doi:10.1152/japplphysiol.00985.2016

3. Camerino GM, Desaphy J-F, De Bellis M, et al. Effects of Nandrolone in the Counteraction of Skeletal Muscle Atrophy in a Mouse Model of Muscle Disuse: Molecular Biology and Functional Evaluation. Guerrero-Hernandez A, ed. *PLOS ONE*. 2015;10(6):e0129686. doi:10.1371/journal.pone.0129686

4. Desaphy J-F, Pierno S, Liantonio A, et al. Antioxidant treatment of hindlimb-unloaded mouse counteracts fiber type transition but not atrophy of disused muscles. *Pharmacol Res*. 2010;61(6):553-563. doi:10.1016/j.phrs.2010.01.012

5. Hyatt H, Deminice R, Yoshihara T, Powers SK. Mitochondrial dysfunction induces muscle atrophy during prolonged inactivity: A review of the causes and effects. *Arch Biochem Biophys*. 2019;662:49-60. doi:10.1016/j.abb.2018.11.005

6. Pierno S, Desaphy JF, Liantonio A, De Bellis M, Bianco G, De Luca A, Frigeri A, Nicchia GP, Svelto M, Léoty C, George AL Jr, Camerino DC. Change of chloride ion channel conductance is an early event of slow-to-fast fibre type transition during unloading-induced muscle disuse. *Brain*. 2002;125(7):1510-1521. doi:10.1093/brain/awf162

7. Desaphy J-F. Skeletal muscle disuse induces fibre type-dependent enhancement of Na+ channel expression. *Brain*. 2001;124(6):1100-1113. doi:10.1093/brain/124.6.1100

8. Brooks NE, Myburgh KH. Skeletal muscle wasting with disuse atrophy is multi-dimensional: the response and interaction of myonuclei, satellite cells and signaling pathways. *Front Physiol*. 2014;5. doi:10.3389/fphys.2014.00099

9. Desaphy J-F, Pierno S, Liantonio A, et al. Recovery of the soleus muscle after short- and long-term disuse induced by hindlimb unloading: effects on the electrical properties and myosin heavy chain profile. *Neurobiol Dis*. 2005;18(2):356-365. doi:10.1016/j.nbd.2004.09.016

10. Foletta VC, White LJ, Larsen AE, Léger B, Russell AP. The role and regulation of MAFbx/atrogin-1 and MuRF1 in skeletal muscle atrophy. *Pflugers Arch*. 2011;461(3):325-335. doi:10.1007/s00424-010-0919-9

11. Ericksen RE, Lim SL, McDonnell E, et al. Loss of BCAA Catabolism during Carcinogenesis Enhances mTORC1 Activity and Promotes Tumor Development and Progression. *Cell Metab*. 2019;29(5):1151-1165.e6. doi:10.1016/j.cmet.2018.12.020

12. Porcelli L, Quatrale AE, Mantuano P, et al. Synergistic antiproliferative and antiangiogenic effects of EGFR and mTOR inhibitors. *Curr Pharm Des*. 2013;19(5):918-926. doi:10.2174/1381612811306050918

30

13. Bodine SC, Stitt TN, Gonzalez M, et al. Akt/mTOR pathway is a crucial regulator of skeletal muscle hypertrophy and can prevent muscle atrophy in vivo. *Nat Cell Biol*. 2001;3(11):1014-1019. doi:10.1038/ncb1101-1014

14. Bifari F, Nisoli E. Branched-chain amino acids differently modulate catabolic and anabolic states in mammals: a pharmacological point of view: Branched-chain amino acids in health and disease. *Br J Pharmacol*. 2017;174(11):1366-1377. doi:10.1111/bph.13624

15. Maki T, Yamamoto D, Nakanishi S, et al. Branched-chain amino acids reduce hindlimb suspension-induced muscle atrophy and protein levels of atrogin-1 and MuRF1 in rats. *Nutr Res*. 2012;32(9):676-683. doi:10.1016/j.nutres.2012.07.005

16. Gannon NP, Schnuck JK, Vaughan RA. BCAA Metabolism and Insulin Sensitivity - Dysregulated by Metabolic Status? *Mol Nutr Food Res*. 2018;62(6):1700756. doi:10.1002/mnfr.201700756

17. D'Antona G, Ragni M, Cardile A, et al. Branched-chain amino acid supplementation promotes survival and supports cardiac and skeletal muscle mitochondrial biogenesis in middle-aged mice. *Cell Metab*. 2010;12(4):362-372. doi:10.1016/j.cmet.2010.08.016

18. Shimomura Y, Yamamoto Y, Bajotto G, et al. Nutraceutical effects of branched-chain amino acids on skeletal muscle. *J Nutr*. 2006;136(2):529S-532S. doi:10.1093/jn/136.2.529S

19. Mantuano P, Bianchini G, Cappellari O, et al. Ergogenic Effect of BCAAs and L-Alanine Supplementation: Proof-of-Concept Study in a Murine Model of Physiological Exercise. *Nutrients*. 2020;12(8). doi:10.3390/nu12082295

20. Moriwaki M, Wakabayashi H, Sakata K, Domen K. The Effect of Branched Chain Amino Acids-Enriched Nutritional Supplements on Activities of Daily Living and Muscle Mass in Inpatients with Gait Impairments: A Randomized Controlled Trial. *J Nutr Health Aging*. 2019;23(4):348-353. doi:10.1007/s12603-019-1172-3

21. Jang J, Yun H-Y, Park J, Lim K. Protective effect of branched chain amino acids on hindlimb suspension-induced muscle atrophy in growing rats. *J Exerc Nutr Biochem*. 2015;19(3):183-189. doi:10.5717/jenb.2015.15062704

22. Silk DB. Proteins, peptides and amino acids: which and when? *Nestle Nutr Workshop Ser Clin Perform Programme*. 2000;3:257-271; discussion 271-274. doi:10.1159/000061812

23. Vig BS, Stouch TR, Timoszyk JK, et al. Human PEPT1 Pharmacophore Distinguishes between Dipeptide Transport and Binding. *J Med Chem*. 2006;49(12):3636-3644. doi:10.1021/jm0511029

24. Willmann R, Lee J, Turner C, et al. Improving translatability of preclinical studies for neuromuscular disorders: lessons from the TREAT-NMD Advisory Committee for Therapeutics (TACT). *Dis Model Mech*. 2020;13(2). doi:10.1242/dmm.042903

25. Capogrosso RF, Mantuano P, Uaesoontrachoon K, et al. Ryanodine channel complex stabilizer compound S48168/ARM210 as a disease modifier in dystrophin-deficient *mdx* mice: proof-of-concept study and independent validation of efficacy. *FASEB J*. 2018;32(2):1025-1043. doi:10.1096/fj.201700182RRR

31

26. Mantuano P, Sanarica F, Conte E, et al. Effect of a long-term treatment with metformin in dystrophic mdx mice: A reconsideration of its potential clinical interest in Duchenne muscular dystrophy. *Biochem Pharmacol*. 2018;154:89-103. doi:10.1016/j.bcp.2018.04.022

27. Mele A, Mantuano P, De Bellis M, et al. A long-term treatment with taurine prevents cardiac dysfunction in mdx mice. *Transl Res*. 2019;204:82-99. doi:10.1016/j.trsl.2018.09.004

28. Sanarica F, Mantuano P, Conte E, et al. Proof-of-concept validation of the mechanism of action of Src tyrosine kinase inhibitors in dystrophic mdx mouse muscle: in vivo and in vitro studies. *Pharmacol Res*. 2019;145:104260. doi:10.1016/j.phrs.2019.104260

29. Capogrosso RF, Mantuano P, Cozzoli A, et al. Contractile efficiency of dystrophic mdx mouse muscle: in vivo and ex vivo assessment of adaptation to exercise of functional end points. *J Appl Physiol*. 2017;122(4):828-843. doi:10.1152/japplphysiol.00776.2015

30. Livak KJ, Schmittgen TD. Analysis of relative gene expression data using real-time quantitative PCR and the 2(-Delta Delta C(T)) Method. *Methods San Diego Calif*. 2001;25(4):402-408. doi:10.1006/meth.2001.1262

31. Wada M, Orihara K, Kamagata M, et al. Circadian clock-dependent increase in salivary IgA secretion modulated by sympathetic receptor activation in mice. *Sci Rep*. 2017;7(1):8802. doi:10.1038/s41598-017-09438-0

32. Cristoni S, Bernardi LR. Bioinformatics in mass spectrometry data analysis for proteomics studies. *Expert Rev Proteomics*. 2004;1(4):469-483. doi:10.1586/14789450.1.4.469

33. Capogrosso RF, Cozzoli A, Mantuano P, et al. Assessment of resveratrol, apocynin and taurine on mechanical-metabolic uncoupling and oxidative stress in a mouse model of duchenne muscular dystrophy: A comparison with the gold standard, α-methyl prednisolone. *Pharmacol Res*. 2016;106:101-113. doi:10.1016/j.phrs.2016.02.016

34. Lescale C, Schenten V, Djeghloul D, et al. Hind limb unloading, a model of spaceflight conditions, leads to decreased B lymphopoiesis similar to aging. *FASEB J Off Publ Fed Am Soc Exp Biol*. 2015;29(2):455-463. doi:10.1096/fj.14-259770

35. Bulankina AV, Thoms S. Functions of Vertebrate Ferlins. *Cells*. 2020;9(3). doi:10.3390/cells9030534

36. Davis DB, Delmonte AJ, Ly CT, McNally EM. Myoferlin, a candidate gene and potential modifier of muscular dystrophy. *Hum Mol Genet*. 2000;9(2):217-226. doi:10.1093/hmg/9.2.217

37. Han S, Cui C, He H, et al. Myoferlin Regulates Wnt/β-Catenin Signaling-Mediated Skeletal Muscle Development by Stabilizing Dishevelled-2 Against Autophagy. *Int J Mol Sci*. 2019;20(20). doi:10.3390/ijms20205130

38. Marimuthu K, Murton AJ, Greenhaff PL. Mechanisms regulating muscle mass during disuse atrophy and rehabilitation in humans. *J Appl Physiol*. 2010;110(2):555-560. doi:10.1152/japplphysiol.00962.2010

39. Bourdeau Julien I, Sephton CF, Dutchak PA. Metabolic Networks Influencing Skeletal Muscle Fiber Composition. *Front Cell Dev Biol*. 2018;6. doi:10.3389/fcell.2018.00125

40. Stelzer JE, Widrick JJ. Effect of hindlimb suspension on the functional properties of slow and fast soleus fibers from three strains of mice. *J Appl Physiol Bethesda Md 1985*. 2003;95(6):2425-2433. doi:10.1152/japplphysiol.01091.2002

41. Aviles H, Belay T, Vance M, Sonnenfeld G. Effects of Space Flight Conditions on the Function of the Immune System and Catecholamine Production Simulated in a Rodent Model of Hindlimb Unloading. *Neuroimmunomodulation*. 2005;12(3):173-181. doi:10.1159/000084850

42. Demonbreun AR, Lapidos KA, Heretis K, et al. Myoferlin regulation by NFAT in muscle injury, regeneration and repair. *J Cell Sci*. 2010;123(Pt 14):2413-2422. doi:10.1242/jcs.065375
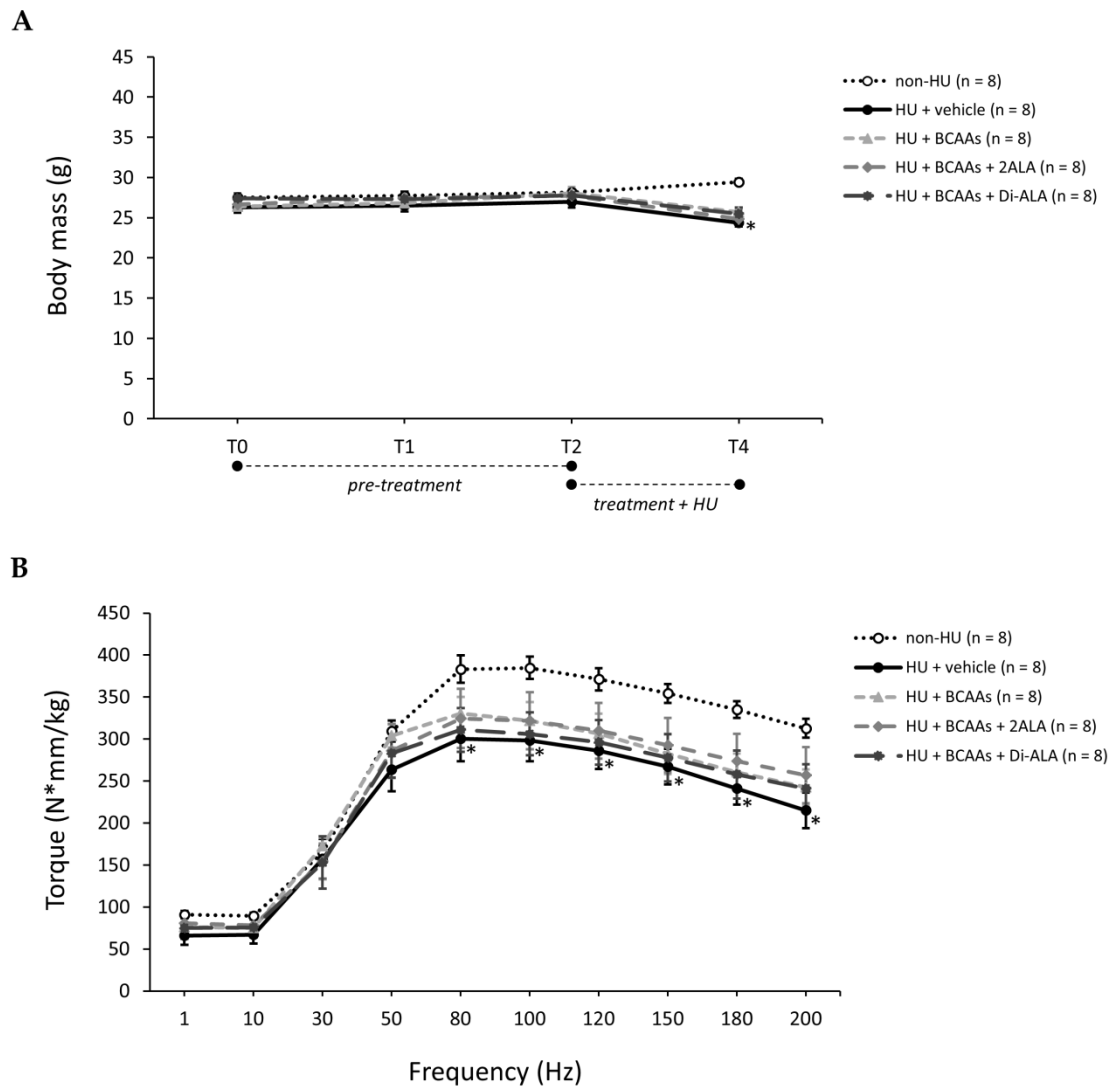
FIGURES

Figure 1

Figure 1.
Scheme illustrating experimental design and timeline of the study.

Figure 2

Figure 2.

In **A** are shown the variations in body mass (g) at time points T0, T1, T2 and T4 for control (non-HU) mice and HU mice treated with vehicle, BCAAs, BCAAs + 2ALA, or BCAAs + Di-ALA. From T0 to T2, mice cohorts underwent a 2-week protocol of pre-treatment preceding the start of hind limb suspension; the treatment continued to be administered for the subsequent two weeks (T2 – T4), in parallel to HU. Both experimental phases are indicated by the dotted lines. Values are expressed as mean ± SEM from the number of mice indicated in brackets. At T4, a statistically significant difference was found by unpaired Student's t-test for HU vs. non-HU mice (*, $p < 0.0001$). No statistically significant differences were found among HU mice groups by one-way ANOVA followed by Dunnett's post hoc test. In **B** are shown the values of *in vivo* hind limb plantar flexor torque (N*mm/kg) produced at increasing stimulation frequencies (from 1 to 200 Hz), obtained from all mice cohorts at T4. Values are expressed as mean ± SEM from the number of mice indicated in brackets. A statistically significant difference was found at frequencies from 80 to 200 Hz by unpaired Student's t-test for HU vs. non-HU mice (*, $0.02 < p < 0.0008$). No statistically significant differences were found among HU mice groups by one-way ANOVA followed by Dunnett's post hoc test.

35

813 **Figure 3**

1
2
3
4
5
6
7
8
9
10
11
12
13
14
15
16
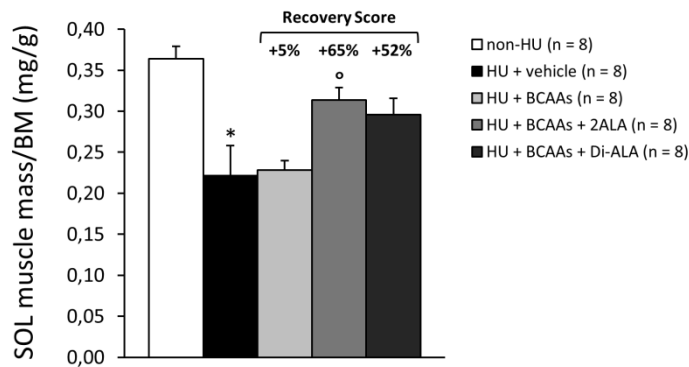
814

815 **Figure 3.**

816 The histogram shows the mass of soleus (SOL) muscle normalized to mice body mass (BM), in mg/g, for
817 non-HU mice and HU mice treated with vehicle, BCAAs, BCAAs + 2ALA, or BCAAs + Di-ALA. Values are
818 expressed as mean ± SEM from the number of mice indicated in brackets. A statistically significant difference
819 was found by unpaired Student's t-test for HU vs. non-HU mice (*, p < 0.007). A statistically significant
820 difference was found among HU mice groups by one-way ANOVA (F = 3.5, p = 0.03). Dunnett's post hoc
821 test, comparing each mixture-treated group to the vehicle group is as follows: °, p < 0.04. The recovery score
822 toward non-HU value calculated for each treated group is indicated above the bars.

823

29
30
31
32
33
34
35
36
37
38
39
40
41
42
43
44
45
46
47
48
49
50
51
52
53
54
55
56
57
58
59
60
61
62
63
64
65

824 **Figure 4**
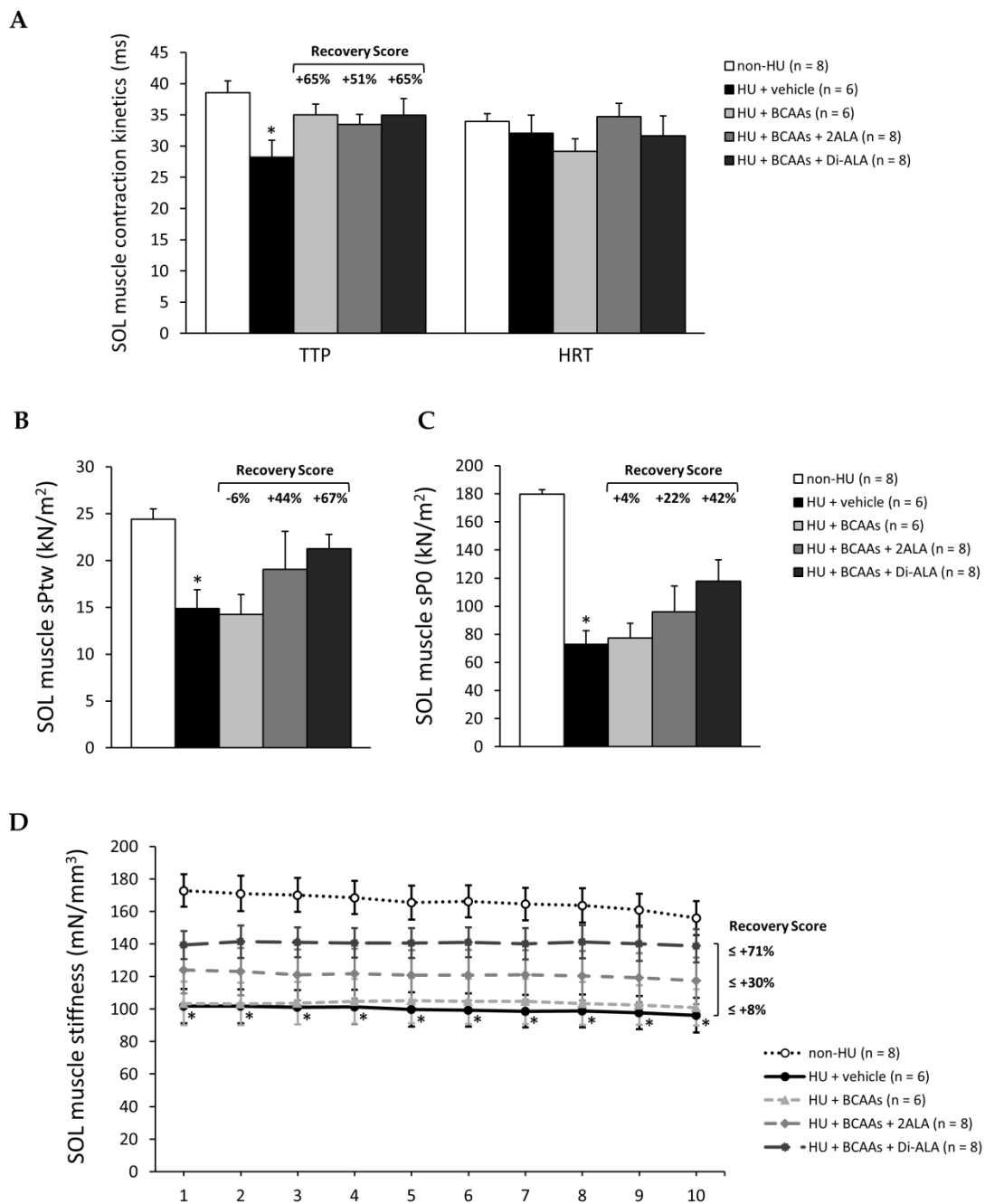
Figure 4.

The graphs show *ex vivo* isometric twitch contraction kinetics (**A**; time to peak, TTP, and half-relaxation time, HRT, both in ms), maximal specific isometric twitch (**B**; sPtw, in kN/m^2) and tetanic (**C**; sP0, in kN/m^2) force values, and elastic properties in response to a series of 10 eccentric pulses (**D**; stiffness, in mN/mm^3), obtained in soleus (SOL) muscles isolated from non-HU mice and HU mice treated with vehicle, BCAAs, BCAAs + 2ALA, or BCAAs + Di-ALA. Values are expressed as mean ± SEM from the number of mice indicated in brackets. For all parameters, a statistically significant difference was found by unpaired Student's t-test for HU vs. non-HU mice (*, $0.001 < p < 0.0001$). No statistically significant differences were found among HU mice groups by one-way ANOVA followed by Dunnett's post hoc test. The recovery score toward non-HU value calculated for each treated group is indicated above the bars for TTP, sPtw and sP0, and at the right end of each line for stiffness.
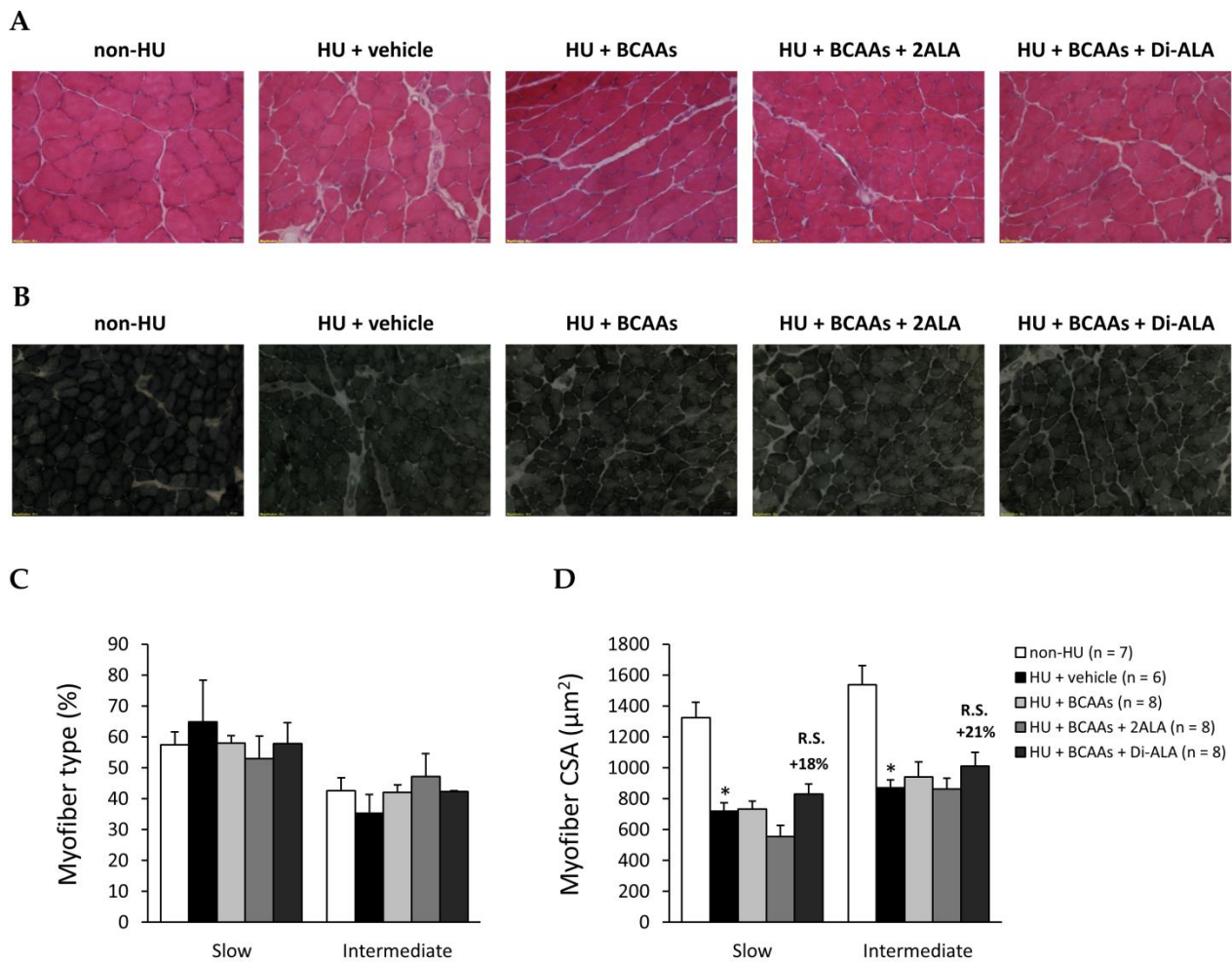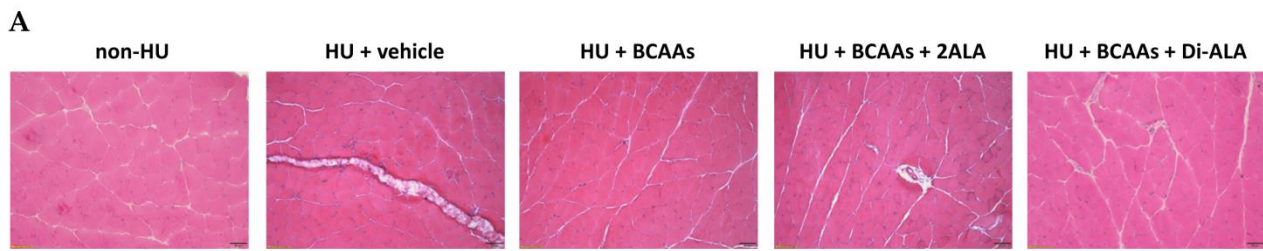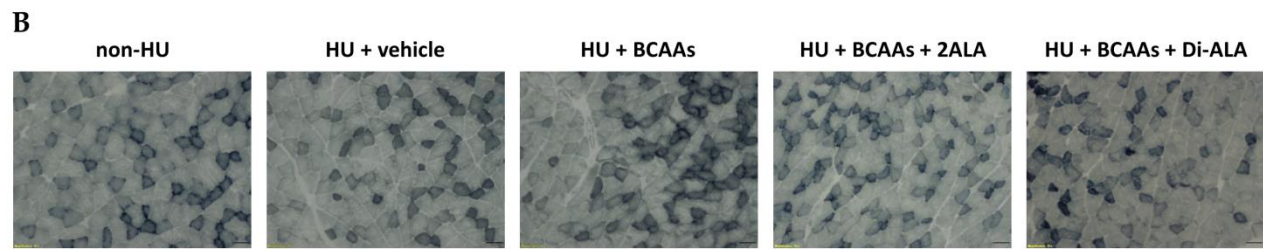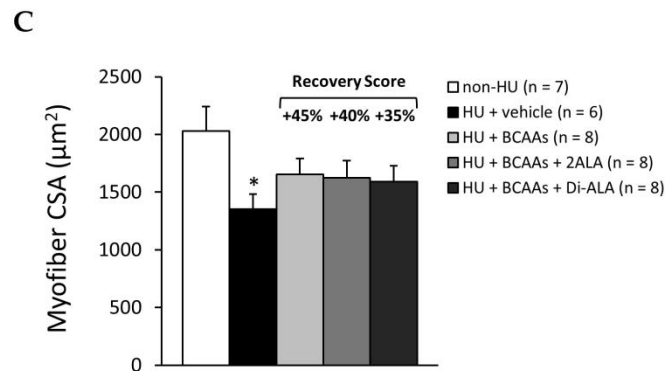
Figure 5

Figure 5.

In **A** are shown representative soleus (SOL) muscle sections stained with hematoxylin and eosin (20× magnification) from non-HU mice and HU mice treated with vehicle, BCAAs, BCAAs + 2ALA, or BCAAs + Di-ALA. This staining allows to appreciate the organization of skeletal muscle architecture and its possible alterations, including the presence of abnormal inflammatory infiltrates or fibrotic areas, quantified via subsequent morphometric analysis. In **B** are shown representative SOL muscle sections stained for succinate dehydrogenase (SDH) histochemistry (10× magnification) for all mice cohorts. This technique allows to distinguish between oxidative (darker) and less oxidative/non-oxidative (lighter) myofibers in each section, due to the different levels of SDH activity. In **C** is shown the mean percentage (%) of each myofiber type (slow and intermediate) with respect to the total number of myofibers (taken as 100%) +/- SEM, while in **D** is shown the cross-sectional area (CSA, µm²) for each myofiber type expressed as mean ± SEM, both obtained from the number of mice indicated in brackets. For myofiber CSA (**D**), a statistically significant difference was found by unpaired Student's t-test for HU vs. non-HU mice, either for slow (*, $p < 0.0004$) and intermediate (*, $p < 0.0006$) fibers. For the CSA of slow fibers, a statistically significant difference was found among HU mice groups by one-way ANOVA (F = 3.7, $p = 0.03$). No individual differences between treated and vehicle groups were found by Dunnett's post hoc test. For myofiber CSA, the recovery score (R.S.) toward non-HU value calculated for the BCAAs + Di-ALA treated group is indicated above the bars.

Figure 6

A

| non-HU | HU + vehicle | HU + BCAAs | HU + BCAAs + 2ALA | HU + BCAAs + Di-ALA |

B

| non-HU | HU + vehicle | HU + BCAAs | HU + BCAAs + 2ALA | HU + BCAAs + Di-ALA |

C
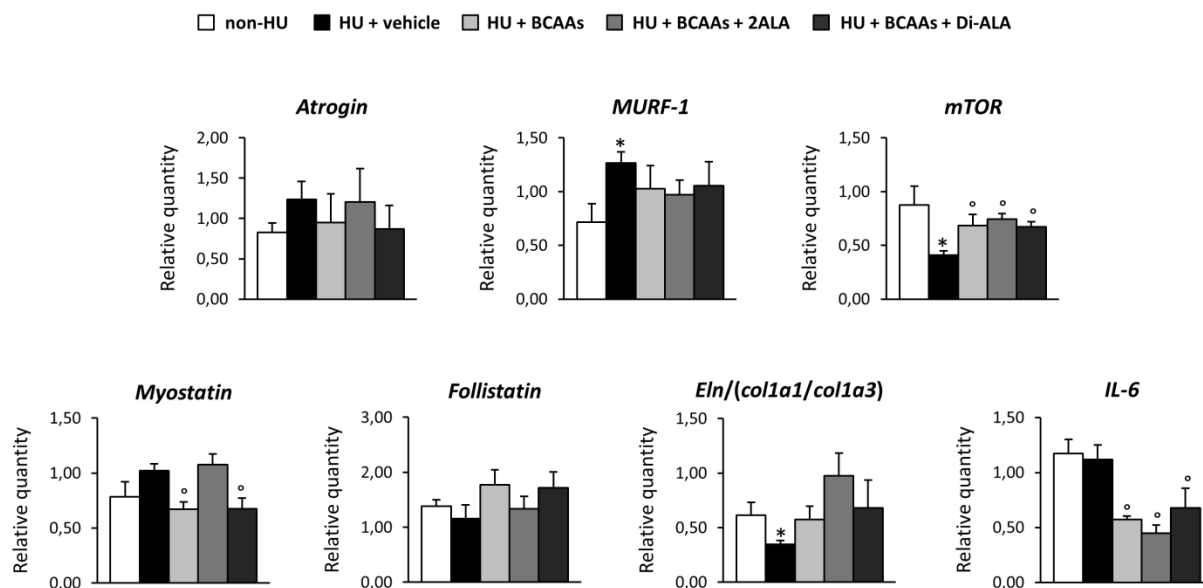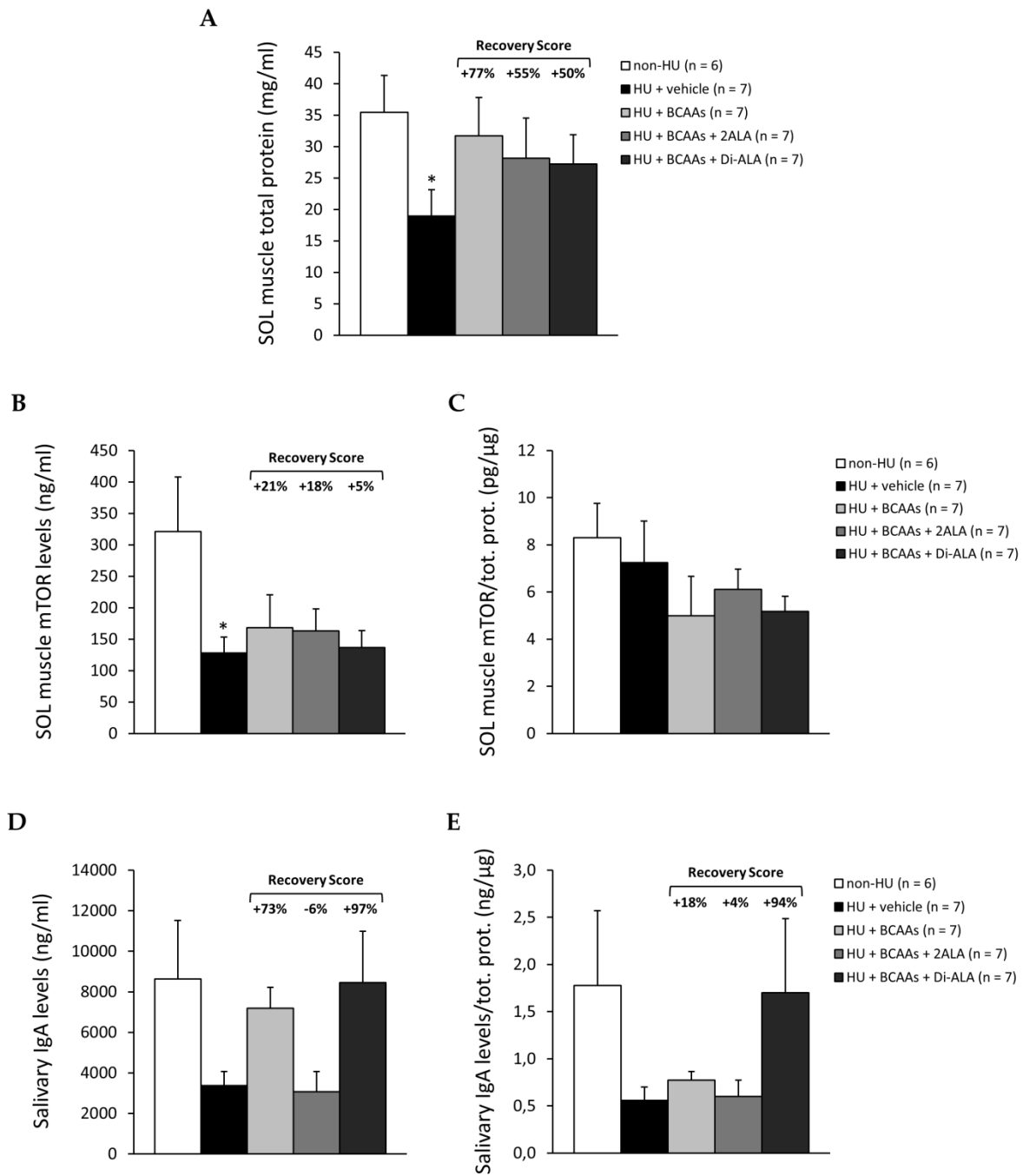

Figure 6.

In **A** are shown representative gastrocnemius (GC) muscle sections stained with hematoxylin and eosin (10× magnification) from non-HU mice and HU mice treated with vehicle, BCAAs, BCAAs + 2ALA, or BCAAs + Di-ALA. This staining allows to appreciate the organization of skeletal muscle architecture and its possible alterations, including the presence of abnormal inflammatory infiltrates or fibrotic areas, quantified via subsequent morphometric analysis. In **B** are shown representative GC muscle sections stained for succinate dehydrogenase (SDH) histochemistry (10× magnification) for all mice cohorts. This technique allows to distinguish between oxidative (darker) and less oxidative/non-oxidative (lighter) myofibers in each section, due to the different levels of SDH activity. In **C** is shown the mean cross-sectional area (CSA, μm^2) for all fiber types (slow, intermediate and fast) +/- SEM, obtained from the number of mice indicated in brackets. A statistically significant difference was found by unpaired Student's t-test for HU vs. non-HU mice (*, $p < 0.03$). No statistically significant differences were found among HU mice groups by one-way ANOVA followed by Dunnett's post hoc test. The recovery score toward non-HU value calculated for each treated group is indicated above the bars.

Figure 7

Figure 7.

The histograms show the transcriptional levels, measured by qRT-PCR in gastrocnemius (GC) muscle, of genes related to skeletal muscle tissue atrophy and growth [*Atrogin-1*, *MuRF-1*, *mTOR*, *Myostatin*, *Follistatin*], elasticity and interactions with extra-cellular matrix [*Elastin*, *Collagen type I α1*, and *Collagen type I α3*, presented as *Eln*/(*col1a1* + *col1a3*) ratio], and inflammation [*IL-6*]. Values are expressed as mean relative quantity ± SEM from 4 – 8 samples *per* group (non-HU mice and HU mice treated with vehicle, BCAAs, BCAAs + 2ALA, BCAAs + Di-ALA), normalized to the mean of housekeeping genes *β-actin*, *HPRT1*, and *TBP*. For *MuRF-1*, *mTOR*, and *Eln*/(*col1a1* + *col1a3*), a statistically significant difference was found by unpaired Student's t-test for HU vs. non-HU mice (*, p < 0.04). A statistically significant difference was found among HU mice groups by one-way ANOVA for *mTOR* (F = 6.1, p = 0.006), *Myostatin* (F = 7.03, p = 0.003), and *IL-6* (F = 6.1, p = 0.004). Dunnett's post hoc test, comparing each mixture-treated group to the vehicle group is as follows: °, 0.002 < p < 0.04.
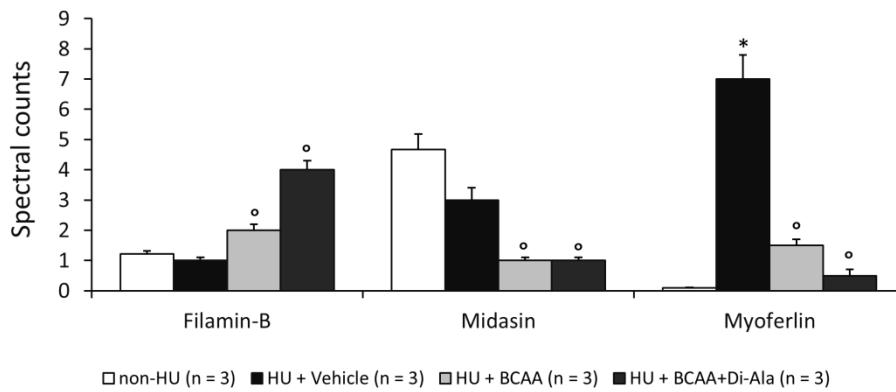
Figure 8

Figure 8.

In **A** is shown the total protein content (mg/ml) measured by Bradford assay in soleus (SOL) muscles from non-HU mice and HU mice treated with vehicle, BCAAs, BCAAs + 2ALA, BCAAs + Di-ALA. In **B** and **C** are shown SOL muscle mTOR protein levels for all mice cohorts, expressed as absolute (**B**; ng/ml) and normalized to total protein (**C**; pg/μg). In **D** and **E** are shown immunoglobulin A (IgA) levels measured in saliva samples collected from mice of each group, expressed as absolute (ng/ml, **D**) and normalized to salivary total protein (ng/μg, **E**). Values are expressed as mean ± SEM from the number of mice indicated in brackets. For **A** and **B**, a statistically significant difference was found by unpaired Student's t-test for HU vs. non-HU mice (*, $p < 0.04$). No statistically significant differences were found among HU mice groups by one-way ANOVA followed by Dunnett's post hoc test. For **A**, **B**, **D**, **E** the recovery score toward non-HU value calculated for each treated group is indicated above the bars.

41

Figure 9

Figure 9.

The figure shows the relative detection intensity (measured as spectral counts) of filamin-B, midasin and myoferlin proteins in plasma samples from non-HU mice and HU mice treated with vehicle, BCAAs, and BCAAs + Di-ALA (n = 3 *per* group). Values are expressed as mean ± SEM from the number of mice indicated in brackets. For myoferlin, a statistically significant difference was found by unpaired Student's t-test for HU vs. non-HU mice (*, $p < 0.001$). A statistically significant difference was found among HU mice groups by one-way ANOVA for filamin-B (F = 50, p = 0.0002), midasin (F = 22.2, p = 0.002), and myoferlin (F = 54.5, p = 0.0001). Dunnett's post hoc test, comparing each mixture-treated group to the vehicle group is as follows: °, $0.0001 < p < 0.03$.

TABLES

Table 1

Formulation	Composition: BCAAs + ALA (Weight Ratio of L-Leu : L-Ile : L-Val : L-ALA/Di-ALA)	Final Dose (mg/kg)
BCAAs	2:1:1	656
BCAAs + 2ALA	2:1:1:2	984
BCAAs + Di-ALA	2:1:1:1	984

Table 1.

In the table are listed the composition the and the daily final dose (mg/kg) of each tested formulation.

Table 2

PK Parameters - AUC (µg/ml*min)			
Group	**L-Valine**	**L-Leucine**	**L-Isoleucine**
BCAAs (n = 6)	5331 ± 428	4639 ± 425	2769 ± 222
BCAAs + 2ALA (n = 6)	7211 ± 698*	5525 ± 548	3247 ± 342
BCAAs + Di-ALA (n = 6)	4955 ± 582	3798 ± 361	2376 ± 242

Table 2.

The table shows the AUC_{0-24} (µg/ml*min) of labelled amino acids for mice treated with BCAAs, BCAAs + 2ALA or BCAAs + Di-ALA. Values are expressed as mean ± SEM from the number of mice *per* group indicated in brackets. Statistically significant differences were found by ANOVA followed by Bonferroni post hoc * vs. BCAAs (F = 11.3, p = 0.03).

Table 3

PK Parameters - MRT (min)			
Group	**L-Valine**	**L-Leucine**	**L-Isoleucine**
BCAAs (n = 6)	76 ± 8	65 ± 7	53 ± 6
BCAAs + 2ALA (n = 6)	108 ± 8	92 ± 6	102 ± 4
BCAAs + Di-ALA (n = 6)	141 ± 20*	135 ± 28**	135 ± 27**

Table 3.

The table shows the MRT (min) concentration of labelled amino acids for mice treated with BCAAs, BCAAs + 2ALA or BCAAs + Di-ALA. Values are expressed as mean ± SEM from the number of mice per group indicated in brackets. Statistically significant differences were found by one-way ANOVA followed by Bonferroni post hoc * vs. BCAAs (F =5.2, p = 0.01 vs. L-Valine, p = 0.007 vs. L-Leucine, p = 0.001 vs. L-Isoleucine).

Table 4

Group	Mass of hind limb muscles/BM (mg/g)				Mass of vital organs/BM (mg/g)			
	GC	TA	EDL	QUAD	Liver	Heart	Kidneys	Spleen
non-HU (n = 8)	5.70 ± 0.13	1.85 ± 0.07	0.36 ± 0.03	7.88 ± 0.16	43.9 ± 1.9	5.81 ± 0.85	6.46 ± 0.17	2.73 ± 0.10
HU + vehicle (n = 8)	5.17 ± 0.29	1.93 ± 0.17	0.38 ± 0.05	7.63 ± 0.39	49.1 ± 1.8	6.41 ± 0.32	7.47 ± 0.24*	2.45 ± 0.10
HU + BCAAs (n = 8)	5.11 ± 0.06	1.87 ± 0.07	0.44 ± 0.05	6.92 ± 0.30	50.7 ± 1.2	5.81 ± 0.17	7.17 ± 0.19	2.54 ± 0.18
HU + BCAAs + 2ALA (n = 8)	5.51 ± 0.40	1.74 ± 0.05	0.29 ± 0.05	7.35 ± 0.31	52.5 ± 0.74	6.15 ± 0.28	7.66 ± 0.38	2.48 ± 0.11
HU + BCAAs + Di-ALA (n = 8)	5.35 ± 0.19	1.98 ± 0.10	0.41 ± 0.02	7.11 ± 0.30	52.3 ± 1.3	5.73 ± 0.12	7.16 ± 0.24	2.63 ± 0.15

Table 4.

The table shows the weight of hind limb gastrocnemius (GC), tibialis anterior (TA), extensor digitorum longus (EDL) and quadriceps (QUAD) muscles, and the weight of organs (liver, heart, kidneys, spleen), normalized to mice body mass (BM), in mg/g, for non-HU mice and HU mice treated with vehicle, BCAAs, BCAAs + 2ALA or BCAAs + Di-ALA. Values are expressed as mean ± SEM from the number of mice indicated in brackets. For kidneys, a statistically significant difference was found by unpaired Student's t-test for HU vs. non-HU mice (*, $p < 0.004$). No statistically significant differences were found among HU mice groups by one-way ANOVA followed by Dunnett's post hoc test.

Table 5

	Muscle histology (H&E staining)							
	SOL muscle (%)				GC muscle (%)			
Group	n	Total damage	Infiltration	Non-muscle	n	Total damage	Infiltration	Non-muscle
non-HU	7	2.82 ± 1.10	1.86 ± 0.60	1.20 ± 0.70	6	3.31 ± 0.30	3.12 ± 0.40	0.19 ± 0.1
HU + vehicle	7	15.6 ± 3.19*	3.23 ± 0.83	10.8 ± 2.50*	4	3.89 ± 0.58	1.99 ± 0.68	1.91 ± 0.67*
HU + BCAAs	7	10.1 ± 1.41	4.37 ± 1.36	6.28 ± 1.22	8	3.05 ± 0.48	1.56 ± 0.22	1.49 ± 0.36
HU + BCAAs + 2ALA	6	9.10 ± 1.98	3.18 ± 0.62	5.92 ± 1.94	8	2.94 ± 1.06	1.56 ± 0.53	1.38 ± 0.59
HU + BCAAs + Di-ALA	6	12 ± 2.06	2.97 ± 0.74	8.46 ± 1.46	7	3.00 ± 0.17	2.28 ± 0.22	0.72 ± 0.38

Table 5.

The table shows the quantitative histological analysis performed on soleus (SOL) and gastrocnemius (GC) muscles' transverse sections stained with hematoxylin and eosin (H&E), for non-HU mice and HU mice treated with vehicle, BCAAs, BCAAs + 2ALA or BCAAs + Di-ALA. In detail, the total area of damage, including the amount of inflammatory cell infiltrates and non-muscle areas (*i.e.* fibrotic and/or adipose tissue), was calculated as average percentage (%) of the total muscle area measured (taken as 100%) +/- SEM from the number of mice indicated for each group (n). Statistically significant differences were found by unpaired Student's t-test for HU vs. non-HU mice (*, $0.003 < p < 0.01$). No statistically significant differences were found among HU mice groups by one-way ANOVA followed by Dunnett's post hoc test.

Conflicts of Interest

The funders conducted the acute pharmacokinetic study (paragraphs 2.1 and 3.1), as well as the plasma proteome and gene ontology study (paragraphs 2.4.8 and 3.3.6), and they had a supporting role in study design, as well as in manuscript revision. All other authors declare no conflict of interest.

Click here to access/download
Supplementary Material
Supplementary materials Mantuano et al._Pharmacol
Res.pptx